Spiral Phases in Doped Antiferromagnets

Diplomarbeit

der Philosophisch-naturwissenschaftlichen Fakultät
der Universität Bern
vorgelegt von

David Baumgartner

2008

Leiter der Arbeit

Prof. Uwe-Jens Wiese

Institut für theoretische Physik, Universität Bern

Abstract

One can create high-temperature superconductors by doping antiferromagnets with holes or electrons. The effective theory that describes such materials in a low-energy regime is the condensed matter analog of chiral perturbation theory in QCD. Using this theory in this work, we study different phases of doped antiferromagnets depending on the values of the low-energy parameters. In order to do so, we investigate the effects of different periodic background field configurations with piecewise constant potentials and compare them to existing results for constant background fields. It will turn out that the energetically most favorable cases are in fact the configurations with constant background fields that were known before.

Ist nicht der Anfang und das Ende
jeder Wissenschaft in Dunkel gehüllt?

Heinrich von Kleist,
Letter to Adolfine von Werdeck

Contents

1 Introduction **1**

2 Low-Energy Effective Field Theory for Magnons and Holes **3**
2.1 Microscopic Models for Antiferromagnets and Their Symmetries 3
2.2 Nonlinear Realization of the $SU(2)_s$ Symmetry 5
2.3 Sublattice Fermion Fields 6
2.4 Fermion Fields in Momentum Space Pockets 8
2.5 Hole Field Identification 9
2.6 Effective Action 10

3 Spirals in the Staggered Magnetization **11**
3.1 Spirals with Uniform Composite Vector Fields 11
3.2 The Energy Density of a Doped Antiferromagnet 12
3.2.1 Magnonic Contribution to the Energy 13
3.2.2 Fermionic Contribution to the Energy 13
3.3 Phases of the Staggered Magnetization 15
3.3.1 Two Populated Hole Pockets 15
3.3.2 Four Populated Hole Pockets 16

4 Investigation of a Piecewise Constant Potential **19**
4.1 Two Filled Hole Pockets 19
4.1.1 Two Sections 19
4.1.2 Three Sections 27
4.1.3 Extrapolation for k Sections 30
4.2 Four Filled Hole Pockets 31
4.2.1 Two Sections 31
4.2.2 Three Sections 34
4.2.3 Extrapolation for k Sections 35

5 Conclusion and Outlook **37**

Acknowledgements **39**

A Construction of the Hamiltonian in Momentum Space **41**

B Construction of the Reciprocal Lattice **47**
B.1 1-Dimensional Case 47
B.2 2-Dimensional Case 49
B.3 The 2-Dimensional Lattice of the Theory 49

C $[D, H] = 0$ for a Periodic Potential $V(x)$ **51**

D Derivatives of $f^f_\pm(E^f_\pm, q, p_2)$ **53**
D.1 Two Sections 53
D.2 Three Sections 54

E Principal Axis Transformation **57**

Bibliography **59**

Chapter 1

Introduction

The phenomenon of low-temperature superconductivity has been known for almost a hundred years. The first successful quantum mechanical explanation was given by Bardeen, Cooper, and Schrieffer in 1957 (BCS theory). In 1986, Bednorz and Müller observed superconductivity in a cuprate material around a critical temperature T_c of 30K. This drew a lot of attention because superconductivity at such high temperatures is not possible in BCS theory. This so-called high-temperature superconductivity has been a matter of intense investigations until today and many materials were found to have this property, some of them even with a critical temperature T_c above 100K. However, until today, the high-temperature superconductivity analog of BCS theory has not yet been found and has therefore remained one of the great puzzles in condensed matter physics.

Superconductivity occurs in hole- or electron-doped antiferromagnetic materials. At low temperature and low doping these materials show antiferromagnetic behavior. As the doping is increased, still at low temperature, the materials enter the superconducting phase. Hence, to be able to understand the superconducting phase, we first investigate the antiferromagnetic phase of a lightly hole-doped system. However, the systematic investigation of the dynamics of holes in an antiferromagnet is complicated due to strong correlations in these systems. Our approach to that problem is the use of a low-energy effective field theory.

The concept of a low-energy effective field theory was originally established by Gasser and Leutwyler in [1] for pions in QCD. Chakravarty, Halperin, and Nelson adapted this concept in [2], describing the low-energy magnon physics by a low-energy effective field theory, the non-linear σ-model. While in QCD the spontaneous breakdown of the chiral symmetry gives rise to the pseudo-Goldstone bosons called pions, in the low-energy physics of cuprates the spontaneous breakdown of the global spin symmetry gives rise to two massless Goldstone bosons, the magnons. However, in the case of the effective field theory for doped antiferromagnets, massive fermions have to be taken into account as well. Therefore, the correct analog in QCD is the baryon chiral perturbation theory, which describes the physics of pions and massive nucleons. Angle resolved photoemission spectroscopy (ARPES) experiments show that in cuprates holes are located inside pockets centered at lattice momenta $\left(\pm\frac{\pi}{2a}, \pm\frac{\pi}{2a}\right)$ [3]. Inspired by baryon chiral perturbation theory, in [4, 5] the pure magnon effective field theory of [6–9] has been extended to a low-energy effective theory for magnons and holes located inside pockets centered at lattice momenta $\left(\pm\frac{\pi}{2a}, \pm\frac{\pi}{2a}\right)$.

The small doping of antiferromagnetic materials causes several experimentally testable effects, such as spirals in the staggered antiferromagnetic magnetization and inhomogeneities in the density of the doping. Well-known inhomogeneous doping configurations are stripes with high and low densities and the so-called checkerboard pattern. The appearance of spirals in the staggered magnetization has also been theoretically predicted in [10–12]. However, it is not known which mechanism causes these effects. For example, we do not know whether long-range Coulomb interactions are necessary for stripe formation. Also, it is controversial whether stripes play a role in the mechanism of high-temperature superconductivity.

Among others, the application of this low-energy effective theory has produced the following results: In [5], the investigation of an antiferromagnet containing two holes in an otherwise undoped system led to bound states with d-wave characteristics. In [13], the focus of the investigations lay on the spatial structure of the staggered magnetization. Using a variational calculation it was found that, depending on the values of the low-energy parameters, spirals in the staggered magnetization indeed occur. They are the zero-degree spiral and the 45° spiral. For another configuration of low-energy parameters, a homogeneous phase of the staggered magnetization was also found. Hence, the question of stability of the spirals against the formation of inhomogeneities arises. In this thesis, we investigate this problem with a generalized variational ansatz, giving the system the freedom to form an inhomogeneous spiral, i.e. stripes, in the staggered magnetization.

This diploma thesis is organized as follows. In chapter 2, we briefly review the microscopic models for antiferromagnets and their symmetries. We then repeat the construction of the low-energy effective field theory for magnons and holes. In chapter 3, we review the appearance of spirals in the staggered magnetization when a constant background field is applied. The case of two filled hole pockets and the case of four filled hole pockets are then discussed explicitly. In chapter 4, we investigate the effect of a periodic background potential with two and three constant sections which will eventually lead us towards a periodic potential with an arbitrarily large number of sections. The calculations are performed for the two-pocket case first and then repeated for the four-pocket case. We will find that in both cases the system prefers a constant background field and hence either a homogeneous phase or a uniform spiral, but no stripes. Finally, chapter 5 contains the conclusions and an outlook.

Chapter 2

Low-Energy Effective Field Theory for Magnons and Holes

In this chapter we review the construction of the low-energy effective field theory according to [5]. In order to do so, the most commonly used models to describe antiferromagnets are introduced first. Their symmetries are of great importance for the further construction of the low-energy effective theories. The symmetries include a general $SU(2)_s$ spin symmetry, the displacement symmetry by one lattice spacing D_i, the 90 degrees rotation O of the quadratic lattice, and the spatial reflection R at the x_1-axis.

The construction of the theory itself is analogous to chiral perturbation in QCD. In QCD the spontaneous breakdown of the $SU(2)_L \otimes SU(2)_R$ chiral symmetry to a $SU(2)_{L=R}$ group gives rise to the pseudo Goldstone bosons called pions. Analogously, in low-energy physics of cuprates the spontaneous breakdown of the global $SU(2)_s$ symmetry down to a local $U(1)_s$ symmetry creates two massless Goldstone bosons, the magnons.

2.1 Microscopic Models for Antiferromagnets and Their Symmetries

The most commonly used microscopic models to describe antiferromagnets are the Hubbard model and the t-J model. To review these models, we first introduce fermion creation and annihilation operators c_{xs} and $c^\dagger_{xs}$ respectively. They obey the standard anticommutation relations

$$\{c^\dagger_{x_i s}, c_{x_j s'}\} = \delta_{ij}\delta_{ss'}, \qquad \{c_{x_i s}, c_{x_j s'}\} = \{c^\dagger_{x_i s}, c^\dagger_{x_j s'}\} = 0. \tag{2.1}$$

For convenience, we express the operators in spinor notation

$$c^\dagger_x = (c^\dagger_{x\uparrow}, c^\dagger_{x\downarrow}), \qquad c_x = \begin{pmatrix} c_{x\uparrow} \\ c_{x\downarrow} \end{pmatrix}. \tag{2.2}$$

Moreover, we introduce the total spin operator $\vec{S}$, which generates the $SU(2)_s$ symmetry

$$\vec{S} = \sum_x \vec{S_x} = \sum_x c^\dagger_x \frac{\vec{\sigma}}{2} c_x, \tag{2.3}$$

denoting the Pauli matrices with $\vec{\sigma}$. In addition to that, we also introduce the charge operator Q

$$Q = \sum_x Q_x = \sum_x (c_x^\dagger c_x - 1) = \sum_x (c_{x\uparrow}^\dagger c_{x\uparrow} + c_{x\downarrow}^\dagger c_{x\downarrow} - 1). \tag{2.4}$$

It is now possible to write down the second quantized Hamiltonian of the Hubbard model

$$H = -t \sum_{x,i} (c_x^\dagger c_{x+\hat{i}} + c_{x+\hat{i}}^\dagger c_x) + \frac{U}{2} \sum_x (c_x^\dagger c_x - 1)^2 - \mu \sum_x (c_x^\dagger c_x - 1). \tag{2.5}$$

In this notation, x denotes the 2-dimensional lattice grid, while $\hat{i}$ denotes a vector of length a, pointing in a lattice direction of a lattice with spacing a. The spins are not fixed at their sites but they are allowed to hop to nearest neighbor sites, if not forbidden by the Pauli principle. Each hop costs a certain amount of energy according to the hopping parameter t. We also have the parameter for the Coulomb repulsion U, $U > 0$, and the chemical potential μ for a fermion-doped lattice relative to a half-filled lattice.

The other important model to describe an antiferromagnet is the t-J model. In our notation the Hamiltonian of that model reads

$$H = P \left\{ -t \sum_{x,i} (c_x^\dagger c_{x+\hat{i}} + c_{x+\hat{i}}^\dagger c_x) + J \sum_{x,i} \vec{S}_x \cdot \vec{S}_{x+\hat{i}} - \mu \sum_x Q_x \right\} P. \tag{2.6}$$

In the t-J model, t represents the hopping parameter and J the exchange coupling constant. For an antiferromagnet, $J > 0$ which favors anti-parallel spin alignment. Due to the projection operator P, the t-J model can only be doped by one spin per site at most.

At this point, it is useful to introduce the following matrix-valued operator, containing the fermion fields

$$C_x = \begin{pmatrix} c_{x\uparrow} & (-1)^x c_{x\downarrow}^\dagger \\ c_{x\downarrow} & -(-1)^x c_{x\uparrow}^\dagger \end{pmatrix}. \tag{2.7}$$

In the following, we shall deal with the relevant transformations of C_x. Under combined transformations $g \in SU(2)_s$ and $\Omega \in SU(2)_Q$ the fermion operator transforms as

$$^{\vec{Q}}C_x = g C_x \Omega^T. \tag{2.8}$$

The displacement operator D_i, shifting the fields one lattice spacing in i-direction, acts as

$$^{D_i}C_x = C_{x+\hat{i}} \sigma_3. \tag{2.9}$$

Furthermore, we need to consider a 90 degrees rotation of the lattice under which the fermion operator transforms as

$$^{O}C_x = C_{Ox}, \tag{2.10}$$

where O transforms a spatial point $x = (x_1, x_2)$ into $Ox = (-x_2, x_1)$. In addition to that, we consider spatial reflection R at the x_1-axis, which turns a spatial point $x = (x_1, x_2)$ into $x = (x_1, -x_2)$. For this symmetry, we get

$$^{R}C_x = C_{Rx}. \tag{2.11}$$

2.2 Nonlinear Realization of the $SU(2)_s$ Symmetry

The staggered magnetization of an antiferromagnet is described by a unit-vector field in spherical coordinates

$$\vec{e}(x) = (\sin\theta(x)\cos\varphi(x), \sin\theta(x)\sin\varphi(x), \cos\theta(x)) \tag{2.12}$$

with $x = (x_1, x_2, t)$ denoting a point in $(2+1)$-dimensional space-time. This vector field lives in the coset space $SU(2)_s/U(1)_s = S^2$. An equivalent $CP(1)$ representation uses 2×2 Hermitean projection matrices that obey

$$P(x) = \frac{1}{2}(\mathbb{1} + \vec{e}(x)\cdot\vec{\sigma}), \quad P(x)^\dagger = P(x), \quad \mathrm{Tr}\,[P(x)] = 1, \quad P(x)^2 = P(x). \tag{2.13}$$

The symmetries of the underlying microscopic models are realized as follows:

$$\begin{aligned}
SU(2)_s: &\qquad P(x)' = gP(x)g^\dagger, \\
D_i: &\qquad {}^{D_i}P(x) = \mathbb{1} - P(x), \\
O: &\qquad {}^{O}P(x) = P(Ox), \qquad Ox = (-x_2, x_1, t), \\
R: &\qquad {}^{R}P(x) = P(Rx), \qquad Rx = (x_1, -x_2, t), \\
T: &\qquad {}^{T}P(x) = \mathbb{1} - P(Tx), \qquad Tx = (x_1, x_2, -t).
\end{aligned} \tag{2.14}$$

In addition to the former transformations, time reversal T is considered here, too.

To construct the nonlinear realization of the $SU(2)_s$ symmetry, one proceeds as follows: First, the magnon field is diagonalized by a unitary transformation $u(x) \in SU(2)$:

$$u(x)P(x)u(x)^\dagger = \frac{1}{2}(\mathbb{1} + \sigma^3) = \begin{pmatrix} 1 & 0 \\ 0 & 0 \end{pmatrix}, \qquad u_{11} \geq 0. \tag{2.15}$$

One obtains

$$u(x) = \begin{pmatrix} \cos\left(\frac{1}{2}\theta(x)\right) & \sin\left(\frac{1}{2}\theta(x)\right)e^{-i\varphi(x)} \\ -\sin\left(\frac{1}{2}\theta(x)\right)e^{i\varphi(x)} & \cos\left(\frac{1}{2}\theta(x)\right) \end{pmatrix}. \tag{2.16}$$

Since the diagonalizing field $u(x)$ transforms under a global transformation $g \in SU(2)_s$ as

$$u(x)' = h(x)u(x)g^\dagger, \qquad u_{11} \geq 0, \tag{2.17}$$

the nonlinear symmetry transformation $h(x)$ is defined implicitly as

$$h(x) = \begin{pmatrix} e^{i\alpha(x)} & 0 \\ 0 & e^{-i\alpha(x)} \end{pmatrix}. \tag{2.18}$$

Under the displacement symmetry D_i, the local staggered magnetization changes sign. Therefore, one obtains

$${}^{D_i}u(x) = \tau(x)u(x), \qquad \tau(x) = \begin{pmatrix} 0 & -e^{-i\varphi(x)} \\ e^{i\varphi(x)} & 0 \end{pmatrix}. \tag{2.19}$$

In order to couple holes to the magnons, the anti-Hermitean traceless field v_μ is introduced

$$v_\mu(x) = u(x)\partial_\mu u(x)^\dagger. \tag{2.20}$$

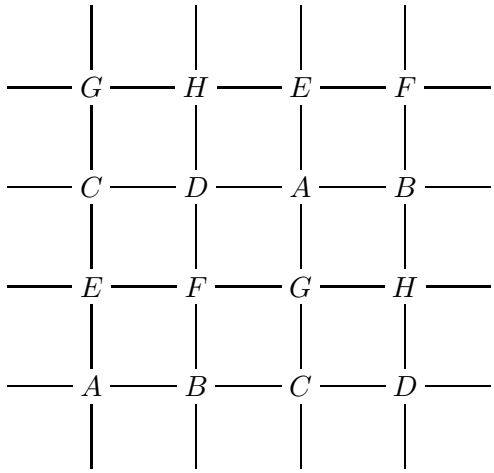

Figure 2.1: Layout and arrangement of the eight sublattices $A, B, ..., H$

The field $v_\mu(x)$ obeys the following transformation rules

$$\begin{aligned}
SU(2)_s: &\qquad v_\mu(x)' = h(x)[v_\mu(x) + \partial_\mu]h(x)^\dagger,\\
D_i: &\qquad {}^{D_i}v_\mu(x) = \tau(x)[v_\mu + \partial_\mu]\tau(x)^\dagger,\\
O: &\qquad {}^{O}v_i(x) = \epsilon_{ij}v_j(Ox),\ {}^{O}v_t = v_t(Ox),\\
R: &\qquad {}^{R}v_1(x) = v_1(Rx),\ {}^{R}v_2(x) = -v_2(Rx),\ {}^{R}v_t(x) = v_t(Rx),\\
T: &\qquad {}^{T}v_j(x) = {}^{D_i}v_j(Tx),\ {}^{T}v_t(x) = -{}^{D_i}v_t(Tx).
\end{aligned} \tag{2.21}$$

Writing

$$v_\mu(x) = iv^a_\mu(x)\sigma_a, \qquad v^\pm_\mu(x) = v^1_\mu(x) \mp iv^2_\mu(x), \tag{2.22}$$

the field $v_\mu(x)$ decomposes into an Abelian gauge field $v^3_\mu(x)$ and two charged vector fields $v^\pm_\mu$, which transform as

$$v^3_\mu(x)' = v^3_\mu(x) - \partial_\mu\alpha(x), \qquad v^\pm_\mu(x)' = v^\pm_\mu(x)e^{\pm 2i\alpha(x)} \tag{2.23}$$

under $SU(2)_s$.

2.3 Sublattice Fermion Fields

At this point, the new lattice operators Ψ^X_x are introduced. They still live on discrete sites of the lattice, relating the transformation rules of the effective fields to those of the microscopic fermion operator matrix C_x, introduced in eq.(2.7). Since in the cuprates the hole pockets reside in the Brillouin zone at lattice momenta $(\pm\frac{\pi}{2a}, \pm\frac{\pi}{2a})$, it is necessary to work with eight sublattices $A, B, ..., H$, which are arranged according to figure 2.1. The lattice operators are constructed as follows

$$\Psi^{A,B,...,H}_x = u(x)C_x, \qquad x \in \{A, B, ..., H\}. \tag{2.24}$$

They inherit the transformation properties from the operators of the Hubbard model

$$\begin{aligned} SU(2)_s: &\qquad \Psi_x^{X\prime} = h(x)\Psi_x^X, \\ D_i: &\qquad {}^{D_i}\Psi_x^X = \tau(x+\hat{i})\Psi_{x+\hat{i}}^{D_iX}\sigma_3, \\ O: &\qquad {}^{O}\Psi_x^X = \Psi_{Ox}^{OX}, \\ R: &\qquad {}^{R}\Psi_x^X = \Psi_{Rx}^{RX}. \end{aligned} \tag{2.25}$$

In the low-energy effective theory a path integral description is used. The electron and hole fields now live in the continuum and are represented by independent Grassmann numbers $\psi_\pm^{A,B,\ldots,H}(x)$ and $\psi_\pm^{A,B,\ldots,H\dagger}(x)$. For convenience, they are combined in the following matrix form

$$\begin{aligned} \Psi^X(x) &= \begin{pmatrix} \psi_+^X(x) & \psi_-^{X\dagger}(x) \\ \psi_-^X(x) & -\psi_+^{X\dagger}(x) \end{pmatrix}, \quad X \in \{A,C,F,H\}, \\ \Psi^X(x) &= \begin{pmatrix} \psi_+^X(x) & -\psi_-^{X\dagger}(x) \\ \psi_-^X(x) & \psi_+^{X\dagger}(x) \end{pmatrix}, \quad X \in \{B,D,E,G\}, \\ \Psi^{X\dagger}(x) &= \begin{pmatrix} \psi_+^{X\dagger}(x) & \psi_-^{X\dagger}(x) \\ \psi_-^X(x) & -\psi_+^X(x) \end{pmatrix}, \quad X \in \{A,C,F,H\}, \\ \Psi^{X\dagger}(x) &= \begin{pmatrix} \psi_+^{X\dagger}(x) & \psi_-^{X\dagger}(x) \\ -\psi_-^X(x) & \psi_+^X(x) \end{pmatrix}, \quad X \in \{B,D,E,G\}. \end{aligned} \tag{2.26}$$

First, it should be noticed that the even sublattices with $X \in \{A,C,F,H\}$ are treated differently than the odd sublattices with $X \in \{B,D,E,G\}$. Furthermore, it has to be pointed out that the matrices $\Psi^{X\dagger}$ consisting of the same Grassmann numbers $\psi_\pm^{A,B,\ldots,H}(x)$ and $\psi_\pm^{A,B,\ldots,H\dagger}(x)$ as $\Psi^X(x)$, do not refer to the conjugate transposed matrices of the according $\Psi^X(x)$. We now define to have the same transformation rules for the matrices $\Psi^X(x)$ and $\Psi^{X\dagger}(x)$ with the fields living in the continuum as for the previous discrete lattice operators Ψ_x^X. In contrast to the lattice operators, however, in the continuum we cannot distinguish between points x and $x+\hat{i}$ anymore. Therefore, the transformation rules take the following form

$$\begin{aligned} SU(2)_s: &\qquad \Psi^X(x)' = h(x)\Psi^X(x), \\ D_i: &\qquad {}^{D_i}\Psi^X(x) = \tau(x)\Psi^{D_iX}, \\ O: &\qquad {}^{O}\Psi^X(x) = \Psi^{Ox}(Ox), \\ R: &\qquad {}^{R}\Psi^X(x) = \Psi^{Rx}(Rx), \\ T: &\qquad {}^{T}\Psi^X(x) = \tau(Tx)(i\sigma_2)[\Psi^{X\dagger}(Tx)^T]\sigma_3, \\ &\qquad {}^{T}\Psi^{X\dagger}(x) = -\sigma_3[\Psi^X(Tx)^T](i\sigma_2)^\dagger\tau(Tx)^\dagger. \end{aligned} \tag{2.27}$$

As we will need the components of the matrices $\Psi_\pm^X(x)$ and $\Psi_\pm^{X\dagger}(x)$ for the further construction of the theory, we also review the transformation properties of the Grassmann numbers $\psi_\pm^X(x)$

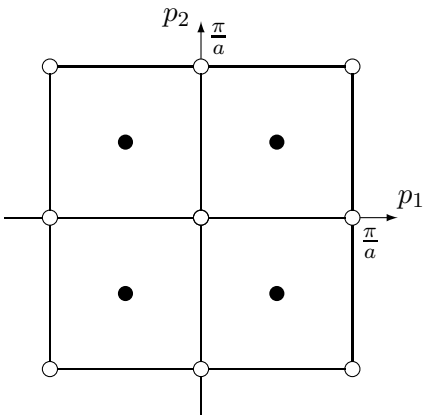

Figure 2.2: The reciprocal lattice with the according momenta and their periodic copies. The black dots represent the momenta $(\pm\frac{\pi}{2a}, \pm\frac{\pi}{2a})$, identifying the location of the center of the hole pockets in the cuprates.

and $\psi_{\pm}^{X\dagger}(x)$

$$\begin{aligned}
SU(2)_s: \quad & \psi_{\pm}^{X}(x)' = e^{\pm i\alpha(x)}\psi_{\pm}^{X}(x), \\
D_i: \quad & {}^{D_i}\psi_{\pm}^{X}(x) = \mp e^{\mp i\varphi(x)}\psi_{\mp}^{D_i X}, \\
O: \quad & {}^{O}\psi_{\pm}^{X}(x) = \psi_{\pm}^{Ox}(Ox), \\
R: \quad & {}^{R}\psi_{\pm}^{X}(x) = \psi_{\pm}^{Rx}(Rx), \\
T: \quad & {}^{T}\psi_{\pm}^{X}(x) = e^{\mp i\varphi(Tx)}\psi_{\pm}^{X\dagger}(Tx), \\
& {}^{T}\psi_{\pm}^{X\dagger}(x) = -e^{\mp i\varphi(Tx)}\psi_{\pm}^{X}(Tx).
\end{aligned} \tag{2.28}$$

2.4 Fermion Fields in Momentum Space Pockets

The eight sublattices $A, B, ..., H$ are dual to eight momenta on the reciprocal lattice shown in figure 2.2. In the cuprates the holes reside in momentum space pockets centered at lattice momenta $(\pm\frac{\pi}{2a}, \pm\frac{\pi}{2a})$. Labelling the momentum space indices

$$k = (k_1, k_2) \in \left\{(0,0), (\frac{\pi}{a}, \frac{\pi}{a}), (\frac{\pi}{a}, 0), (0, \frac{\pi}{a}), (\pm\frac{\pi}{2a}, \pm\frac{\pi}{2a})\right\}, \tag{2.29}$$

and using the Grassmann numbers $\psi_{\pm}^{X}(x)$, the following new fields are constructed

$$\begin{aligned}
\psi_{\pm}^{k}(x) &= \frac{1}{\sqrt{8}}\sum_{X} e^{ikx}\psi_{\pm}^{X}(x) \\
&= \frac{1}{\sqrt{8}}\Big\{\psi_{\pm}^{A}(x) + e^{-ik_1 a}\psi_{\pm}^{B}(x) + e^{-2ik_1 a}\psi_{\pm}^{C}(x) + e^{-3ik_1 a}\psi_{\pm}^{D}(x) \\
&\qquad + e^{-ik_2 a}\left[\psi_{\pm}^{E}(x) + e^{-ik_1 a}\psi_{\pm}^{F}(x) + e^{-2ik_1 a}\psi_{\pm}^{G}(x) + e^{-3ik_1 a}\psi_{\pm}^{H}(x)\right]\Big\}
\end{aligned} \tag{2.30}$$

They transform as

$$\begin{aligned}
SU(2)_s: &\qquad \psi^k_\pm(x)' = e^{\pm i\alpha(x)}\psi^k_\pm(x)\\
D_i: &\qquad {}^{D_i}\psi_\pm(x) = \mp e^{ik_i a}e^{\mp\varphi(x)}\psi^k_\mp(x)\\
O: &\qquad {}^{O}\psi^k_\pm(x) = \psi^{Ok}_\pm(Ox)\\
R: &\qquad {}^{R}\psi^k_\pm(x) = \psi^{Rk}_\pm(Rx)\\
T: &\qquad {}^{T}\psi^k_\pm(x) = e^{\pm i\varphi(Tx)}\psi^{-k\dagger}_\pm(Tx)\\
&\qquad {}^{T}\psi^{k\dagger}_\pm(x) = e^{\pm i\varphi(Tx)}\psi^{-k}_\pm(Tx).
\end{aligned} \tag{2.31}$$

2.5 Hole Field Identification

Until here, the theory contains both hole and electron fields. From now on, only holes but not electrons shall be considered as charge carriers. Therefore, the electron fields have to be eliminated from the theory.

Through a mass term a field $\psi^k_\pm$ with lattice momentum k can only mix with fields having the same lattice momentum k or one specific different momentum k'. Therefore, the eight lattice momenta can be divided into four pairs. In cuprates, the holes are centered at the following lattice momenta

$$k^\alpha = (\frac{\pi}{2a},\frac{\pi}{2a}), \qquad k^{\alpha'} = -k^\alpha, \qquad k^\beta = (\frac{\pi}{2a},-\frac{\pi}{2a}), \qquad k^{\beta'} = -k^\beta. \tag{2.32}$$

Due to the transformation rules of eq.(2.31) the following invariant mass terms can be constructed

$$\sum_{f=\alpha,\beta}\left[(\psi^{k^f\dagger}_+,\psi^{k^{f'}\dagger}_+)\begin{pmatrix} m & \mathcal{M}\\ \mathcal{M} & m\end{pmatrix}\begin{pmatrix}\psi^{k^f}_+\\ \psi^{k^{f'}}_+\end{pmatrix} + (\psi^{k^f\dagger}_-,\psi^{k^{f'}\dagger}_-)\begin{pmatrix} m & -\mathcal{M}\\ -\mathcal{M} & m\end{pmatrix}\begin{pmatrix}\psi^{k^f}_-\\ \psi^{k^{f'}}_-\end{pmatrix}\right]. \tag{2.33}$$

The different masses m and $\mathcal{M}$ are due to different terms of which the ones proportional to the mass $\mathcal{M}$ are invariant under $SU(2)_Q$ transformations while the terms proportional to m are invariant only under $U(1)_Q$ transformations. By diagonalizing the mass matrices, it is possible to identify particle and hole fields. The eigenvalues of the matrix are $m\pm\mathcal{M}$. The particles correspond to states with eigenvalue $m+\mathcal{M}$ and holes correspond to states with the lower eigenvalue $m-\mathcal{M}$. For the hole fields, we identify the according eigenvectors as

$$\psi^f_+(x) = \frac{1}{\sqrt{2}}\left[\psi^{k^f}_+(x) - \psi^{k^{f'}}_+(x)\right], \qquad \psi^f_-(x) = \frac{1}{\sqrt{2}}\left[\psi^{k^f}_-(x) - \psi^{k^{f'}}_-(x)\right]. \tag{2.34}$$

Under the various symmetries the hole fields $\psi^f_\pm$, $f\in\{\alpha,\beta\}$, transform as

$$\begin{aligned}
SU(2)_s: &\qquad \psi^f_\pm(x)' = e^{\pm i\alpha(x)}\psi^f_\pm(x)\\
D_i: &\qquad {}^{D_i}\psi^f_\pm(x) = \mp e^{ik^f_i a}e^{\mp\varphi(x)}\psi^f_\mp(x)\\
O: &\qquad {}^{O}\psi^\alpha_\pm(x) = \mp\psi^\beta_\pm(Ox), \qquad {}^{O}\psi^\beta_\pm(x) = \mp\psi^\alpha_\pm(Ox),\\
R: &\qquad {}^{R}\psi^\alpha_\pm(x) = \psi^\beta_\pm(Rx), \qquad {}^{R}\psi^\beta_\pm(x) = \psi^\alpha_\pm(Rx),\\
T: &\qquad {}^{T}\psi^f_\pm(x) = \pm e^{\mp i\varphi(Tx)}\psi^{f\dagger}_\pm(Tx)\\
&\qquad {}^{T}\psi^{f\dagger}_\pm(x) = \mp e^{\pm i\varphi(Tx)}\psi^f_\pm(Tx).
\end{aligned} \tag{2.35}$$

The effective action of the theory must then be invariant under these transformations.

2.6 Effective Action

The low-energy effective action of magnons and holes is constructed as a derivative expansion. At low energies, terms with a small number of derivatives dominate. In the case of heavy non-relativistic fermions, one time-derivative counts like two spatial derivatives. Each term must be consistent with the symmetries listed in eq.(2.35). In a general form, the effective action is written as

$$S[\psi_{\pm}^{f\dagger}, \psi_{\pm}^{f}, P] = \int d^2x \; dt \sum_{n_\psi} \mathcal{L}_{n_\psi}. \tag{2.36}$$

In this notation, n_ψ denotes the necessarily even number of fermion fields that the various terms contain. The leading terms in the pure magnon sector are

$$\mathcal{L}_0 = \rho_s \mathrm{Tr}\left[\partial_i P \partial_i P + \frac{1}{c^2}\partial_t P \partial_t P\right], \tag{2.37}$$

with the spin stiffness ρ_s and the spinwave velocity c. The leading order terms with two fermion fields containing at most one temporal or two spatial derivatives read

$$\begin{aligned}\mathcal{L}_2 = \sum_{\substack{f=\alpha,\beta \\ s=+,-}} \Big[& M\psi_s^{f\dagger}\psi_s^f + \psi_s^{f\dagger} D_t \psi_s^f \\ & + \frac{1}{2M'} D_i\psi_s^{f\dagger} D_i \psi_s^f + \sigma_f \frac{1}{2M''}\left(D_1\psi_s^{f\dagger} D_2\psi_s^f + D_2\psi_s^{f\dagger} D_1\psi_s^f\right) \\ & + \Lambda\left(\psi_s^{f\dagger} v_1^s \psi_{-s}^f + \sigma_f \psi_s^{f\dagger} v_2^s \psi_{-s}^f\right) \\ & + N_1 \psi_s^{f\dagger} v_i^s v_i^{-s} \psi_{-s}^f + \sigma_f N_2\left(\psi_s^{f\dagger} v_1^s v_2^{-s}\psi_s^f + \psi_s^{f\dagger} v_2^s v_1^{-s}\psi_s^f\right)\Big].\end{aligned} \tag{2.38}$$

Here, M denotes the rest mass of a hole, while M' and M'' are kinetic mass parameters, Λ is a hole-one-magnon, and N_1 and N_2 are hole-two-magnon couplings. All these parameters take real values. The parameter σ_f takes the value $\sigma_\alpha = +1$ for $f = \alpha$ and $\sigma_\beta = -1$ for $f = \beta$. The covariant derivative D_μ reads

$$D_\mu \psi_{\pm}^f(x) = \partial_\mu \psi_{\pm}^f(x) \pm i v_\mu^3(x) \psi_{\pm}^f. \tag{2.39}$$

The Lagrangian with four fermion fields $\mathcal{L}_4$ can be found in [5]. We will neither treat four-fermion couplings nor higher order terms in this work.

Chapter 3

Spirals in the Staggered Magnetization

In this chapter we first review the reason for the possible appearance of spirals in the staggered magnetization. Moreover, we review the concept of how to construct the total energy density of a doped antiferromagnet. We then derive from that the configuration of the staggered magnetization in the cases of either two or four filled hole pockets.

3.1 Spirals with Uniform Composite Vector Fields

Henceforth, we will show how spirals in the staggered magnetization arise. In this discussion, only time-independent configurations of the background field with $v_t(x) = 0$ shall be considered.

The holes couple to the composite vector field $v_i(x)$ in a gauge covariant way. We assume $v_i(x)$ to be constant up to a gauge transformation. We thus have

$$\begin{aligned} v_i^3(x)' &= v_i^3(x) - \partial_i \alpha(x) = c_i^3, \\ v_i^\pm(x)' &= v_i^\pm(x) e^{\pm 2i\alpha(x)} = c_i^\pm, \end{aligned} \tag{3.1}$$

with c_i^3 and $c_i^\pm$ being constant. By an appropriate gauge transformation, one can always achieve

$$c_i^+ = c_i^- = c_i, \qquad c_i \in \mathbb{R}. \tag{3.2}$$

Using the definition of the unit-vector field in eq.(2.12), the equations (3.1) can be expressed in dependence of $\theta(x)$ and $\varphi(x)$,

$$\begin{aligned} v_i^3(x)' &= \sin^2 \frac{\theta(x)}{2} \partial_i \varphi(x) - \partial_i \alpha(x) = c_i^3, \\ v_i^\pm(x)' &= \frac{1}{2} \left[\sin\theta(x) \partial_i \varphi(x) \pm i \partial_i \theta(x) \right] e^{\mp i(\varphi(x) - 2\alpha(x))} = c_i^\pm. \end{aligned} \tag{3.3}$$

Considering the following class of configurations

$$\theta(x) = \theta_0, \qquad \varphi(x) = k_i x_i, \tag{3.4}$$

and a gauge transformation

$$\alpha(x) = \frac{1}{2} k_i x_i, \tag{3.5}$$

one indeed obtains constant fields c_i and c_i^3

$$\begin{aligned} v_i^3(x)' &= k_i \left(\sin^2 \frac{\theta_0}{2} - \frac{1}{2} \right) = -\frac{k_i}{2} \cos\theta_0 = c_i^3, \\ v_i^{\pm}(x)' &= \frac{k_i}{2} \sin\theta_0 = c_i, \\ v_t(x)' &= 0. \end{aligned} \tag{3.6}$$

This set of background fields corresponds to different configurations for the vector field $\vec{e}(x)$, depending on the low-energy parameters that govern the filling of the hole pockets.

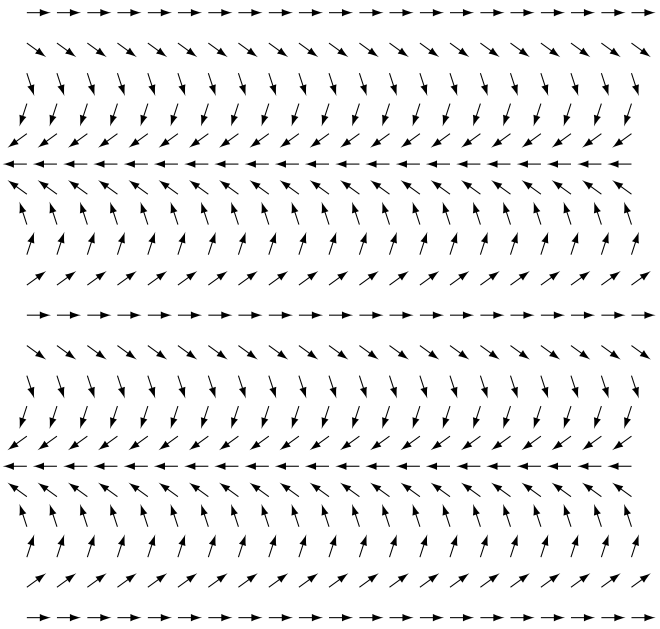

Figure 3.1: Example of a spiral in the staggered magnetization. The example is a homogeneous zero degree spiral along the x_2-axis as it may occur in the case of two filled hole pockets. The corresponding calculations are shown in subsection 3.3.1.

3.2 The Energy Density of a Doped Antiferromagnet

The energy density of an undoped antiferromagnet is ϵ_0. In a doped antiferromagnet, however, the energy density is modified by a magnonic part ϵ_m and a fermionic part ϵ_h. The total energy density in a doped antiferromagnet then reads

$$\epsilon = \epsilon_0 + \epsilon_m + \epsilon_h. \tag{3.7}$$

The following two subsections deal with the construction of the magnonic and the fermionic contribution of the energy density.

3.2.1 Magnonic Contribution to the Energy

The leading terms of the energy density in the pure magnon sector correspond to the first term of the Lagrangian $\mathcal{L}_0$ introduced in eq.(2.37)

$$\epsilon_m = \rho_s \mathrm{Tr}\left[\partial_i P \partial_i P\right] = \frac{\rho_s}{2} \partial_i \vec{e}(x) \cdot \partial_i \vec{e}(x).$$

With a gauge transformation as suggested in eq.(3.1), such that $c_i^+ = c_i^- = c_i$, the magnonic contribution to the energy density ϵ_m can be determined as

$$\epsilon_m = \frac{\rho_s}{2} \partial_i \vec{e}(x) \cdot \partial_i \vec{e}(x) = 2\rho_s (c_1^2 + c_2^2). \tag{3.8}$$

3.2.2 Fermionic Contribution to the Energy

The fermionic contribution is calculated as follows: The parameters c_i^3 and $c_i^\pm$ are fixed. In addition to that, the hole-two-magnon vertices proportional to N_1 and N_2 are neglected because they involve two spatial derivatives and are thus of higher order than the hole-one-magnon vertex proportional to Λ. The Hamiltonian derived from eq.(2.38) then reads

$$\begin{aligned} H = \int d^2x \sum_{\substack{f=\alpha,\beta \\ s=+,-}} \Big[& M \Psi_s^{f\dagger} \Psi_s^f + \frac{1}{2M'} D_i \Psi_s^{f\dagger} D_i \Psi_s^f \\ & + \sigma_f \frac{1}{2M''} (D_1 \Psi_s^{f\dagger} D_2 \Psi_s^f + D_2 \Psi_s^{f\dagger} D_1 \Psi_s^f) \\ & + \Lambda (\Psi_s^{f\dagger} v_1^s \Psi_{-s}^f + \sigma_f \Psi_s^{f\dagger} v_2^s \Psi_{-s}^f) \Big], \end{aligned} \tag{3.9}$$

with the covariant derivative

$$D_i \Psi_\pm^f(x) = \partial_i \Psi_\pm^f(x) \pm i v_i^3(x) \Psi_\pm^f(x). \tag{3.10}$$

In this Hamiltonian, $\Psi_s^{f\dagger}(x)$ and $\Psi_s^f(x)$ are creation and annihilation operators (and no longer Grassman numbers) for fermions of flavor $f = \alpha, \beta$ and spin $s = +, -$. In this case, the indices plus and minus refer to spins aligned parallel or anti-parallel to the local staggered magnetization, respectively. The operators obey standard canonical anti-commutation relations. After a gauge transformation according to eq.(3.1), the fermions experience a constant composite vector field. Switching to momentum space and considering that the flavors α and β do not mix, the Hamiltonian can be written as

$$H^f(p) = \begin{pmatrix} M + \frac{(p_i - c_i^3)^2}{2M'} + \sigma_f \frac{(p_1 - c_1^3)(p_2 - c_2^3)}{M''} & \Lambda(c_1 + \sigma_f c_2) \\ \Lambda(c_1 + \sigma_f c_2) & M + \frac{(p_i + c_i^3)^2}{2M'} + \sigma_f \frac{(p_1 + c_1^3)(p_2 + c_2^3)}{M''} \end{pmatrix}. \tag{3.11}$$

A mathematical derivation of this Hamiltonian can be found in appendix A. The diagonalization of the Hamiltonian leads to the energy-momentum dispersion relation

$$\begin{aligned} E_\pm^f(p) \;=\; & M + \frac{p_i^2 + (c_i^3)^2}{2M'} + \sigma_f \frac{p_1 p_2 + c_1^3 c_2^3}{M''} \\ & \pm \sqrt{\left(\frac{p_i c_i^3}{M'} + \sigma_f \frac{p_1 c_2^3 + p_2 c_1^3}{M''} \right)^2 + \Lambda^2 (c_1 + \sigma_f c_2)^2}. \end{aligned} \tag{3.12}$$

It needs to be pointed out that in this notation the indices plus and minus no longer refer to the spin orientation, but to a higher energy level E^f_+ and a lower energy level E^f_-. Indeed, the eigenvectors corresponding to $E^f_\pm$ are linear combinations of both spin orientations. The minimum of the energy is located at $p = 0$. In that case, the dispersion relation reads

$$E^f_\pm(0) = M + \frac{(c^3_i)^2}{2M'} + \sigma_f \frac{c^3_1 c^3_2}{M''} \pm \Lambda|c_1 + \sigma_f c_2|. \tag{3.13}$$

Due to eq.(3.8), the parameters c^3_i do not affect the magnonic contribution to the energy density. We therefore fix them by minimizing the energy $E^f_-(0)$ with respect to c^3_1 and c^3_2. It turns out that $c^3_1 = c^3_2 = 0$ and in this case the dispersion relation eq.(3.12) is reduced to

$$E^f_\pm(p) = M + \frac{p^2_i}{2M'} + \sigma_f \frac{p_1 p_2}{M''} \pm \Lambda|c_1 + \sigma_f c_2|. \tag{3.14}$$

Thus, the filled hole pockets $P^f_\pm$ are ellipses

$$\frac{p^2_i}{2M'} + \sigma_f \frac{p_1 p_2}{M''} = T^f_\pm \tag{3.15}$$

with the kinetic energy $T^f_\pm$ of the hole pocket $P^f_\pm$ at the Fermi surface. The area of the occupied hole pocket determines the fermion density. The fermion density is thus identified as

$$n^f_\pm = \frac{1}{(2\pi)^2} \int_{P^f_\pm} d^2p = \frac{1}{2\pi} M_{\text{eff}} T^f_\pm, \tag{3.16}$$

with the effective mass M_{eff}

$$M_{\text{eff}} = \frac{M'M''}{\sqrt{M''^2 - M'^2}}. \tag{3.17}$$

The kinetic energy density of a filled pocket is given by

$$t^f_\pm = \frac{1}{(2\pi)^2} \int_{P^f_\pm} d^2p \; T^f_\pm = \frac{1}{4\pi} M_{\text{eff}} {T^f_\pm}^2. \tag{3.18}$$

The total fermion density for fermions of all flavors is then calculated as

$$n = n^\alpha_+ + n^\alpha_- + n^\beta_+ + n^\beta_- = \sum_{\substack{f=\alpha,\beta \\ s=+,-}} n^f_s. \tag{3.19}$$

The above results are now used to calculate the total energy density of the holes

$$\epsilon_h = \epsilon^\alpha_+ + \epsilon^\alpha_- + \epsilon^\beta_+ + \epsilon^\beta_- = \sum_{\substack{f=\alpha,\beta \\ s=+,-}} \epsilon^f_s, \tag{3.20}$$

with the energy density $\epsilon^f_\pm$ of one hole

$$\epsilon^f_\pm = (M \pm \Lambda|c_1 + \sigma_f c_2|) n^f_\pm + t^f_\pm. \tag{3.21}$$

The filling of the pockets is determined by the kinetic energy and thus by the parameters $T^f_\pm$. They must be varied in order to minimize the total energy density. In addition to that,

the total density of the holes n is fixed. Hence, we hence have a variational problem with constraints and therefore introduce the Lagrange multiplier μ to fix the density n

$$S = \epsilon_h - \mu n. \tag{3.22}$$

The variation demands

$$\begin{aligned}
\frac{\partial S}{\partial T_\pm^f} &= \frac{\partial}{\partial T_\pm^f}(\epsilon_h - \mu n) \\
&= \frac{\partial}{\partial T_\pm^f}\left((M \pm \Lambda|c_1 + \sigma_f c_2|)n + \sum_{\substack{f=\alpha,\beta \\ s=+,-}} t_\pm^f - \mu n\right) \\
&= \frac{\partial}{\partial T_\pm^f}\left(\frac{1}{2\pi}M_{\text{eff}}(M \pm \Lambda|c_1 + \sigma_f c_2| - \mu)\sum_{\substack{f=\alpha,\beta \\ s=+,-}} T_\pm^f + \frac{1}{4\pi}M_{\text{eff}}\sum_{\substack{f=\alpha,\beta \\ s=+,-}} {T_\pm^f}^2\right) \\
&= \frac{1}{2\pi}M_{\text{eff}}(M \pm \Lambda|c_1 + \sigma_f c_2| + T_\pm^f - \mu) \\
&\stackrel{!}{=} 0.
\end{aligned} \tag{3.23}$$

3.3 Phases of the Staggered Magnetization

It is now possible to populate various hole pockets with holes. For each case, one varies the parameters $T_\pm^f$ in order to minimize the energy of the fermions. To minimize the total energy density, one then minimizes the parameters c_i of the magnon field. Depending on how many pockets are filled, different configurations of the staggered magnetization are then established. Careful investigations on that subject have been carried out in [13]. They show that for three populated pockets as well as for one populated pocket there are always energetically more favorable cases. They are, depending on the low-energy parameters, either the four-pocket case which produces a homogeneous configuration of the staggered magnetization, or the two-pocket case causing a field configuration with a homogeneous zero degree spiral. In chapter 4, the influence of a piecewise constant potential on the staggered magnetization for both two and four filled pockets is investigated. Therefore, in this section these configurations are reviewed in detail in the case of a constant potential c_i in both the x_1 and the x_2-direction.

3.3.1 Two Populated Hole Pockets

If two pockets are filled with holes, necessarily only the pockets with lower energies are populated and we therefore need to consider the pockets with energies E_-^α and E_-^β. We thus have a hole density

$$n = n_-^\alpha + n_-^\beta = \frac{1}{2\pi}M_{\text{eff}}\left(T_-^\alpha + T_-^\beta\right) \tag{3.24}$$

and a fermionic energy density

$$\epsilon_h = \epsilon_-^\alpha + \epsilon_-^\beta. \tag{3.25}$$

The variation according to eq.(3.23) then yields

$$\begin{aligned} \mu &= M + \frac{\pi n}{M_{\text{eff}}} - \frac{\Lambda}{2}(|c_1 + c_2| + |c_1 - c_2|), \\ T_-^f &= \frac{\Lambda}{2}(|c_1 + c_2| - \sigma_f |c_1 - c_2|). \end{aligned} \tag{3.26}$$

In that case, the total energy density reads

$$\begin{aligned} \epsilon &= \epsilon_0 + \epsilon_m + \epsilon_h \\ &= \epsilon_0 + 2\rho_s(c_1^2 + c_2^2) + \left(M - \frac{\Lambda}{2}(|c_1 + c_2| + |c_1 - c_2|) \right) n + \frac{\pi n^2}{2M_{\text{eff}}} \\ &\quad - \frac{1}{2\pi} M_{\text{eff}} \frac{\Lambda^2}{4} (|c_1 + c_2| - |c_1 - c_2|)^2. \end{aligned} \tag{3.27}$$

This configuration is stable for $2\pi\rho_s > \frac{1}{2} M_{\text{eff}} \Lambda^2$. The energy density is then bounded from below with its minimum at

$$|c_1| = \frac{\Lambda}{4\rho_s} n, \; |c_2| = 0, \qquad \text{or} \qquad |c_1| = 0, \; |c_2| = \frac{\Lambda}{4\rho_s} n. \tag{3.28}$$

Comparing this result with eq.(3.6), we find the following vector field configuration: Since the parameters c_i^3 have been set to zero earlier, $\cos\theta_0 = 0$. Hence $\theta_0 = \pm\frac{\pi}{2}$ and every vector of the unit-vector field $\vec{e}(x)$ points to the equator of the unit sphere. Furthermore, according to the two solutions in eq.(3.28), it is obvious that either $k_1 = 0$ or $k_2 = 0$. Therefore, the direction of the unit-vector field is either independent of x_1 or x_2 and spirals along either axes x_2 or x_1 arise, respectively. They are called zero-degree spirals and we have already seen an example in figure 3.1.

3.3.2 Four Populated Hole Pockets

If four pockets are filled with holes, however, we need to consider hole pockets filled with holes of both flavors α and β as well as both energies E_+^f and E_-^f. The according hole density is thus

$$n = n_-^\alpha + n_+^\alpha + n_-^\beta + n_+^\beta = \frac{1}{2\pi} M_{\text{eff}} \left(T_-^\alpha + T_+^\alpha + T_-^\beta + T_+^\beta \right), \tag{3.29}$$

and the fermionic energy density is

$$\epsilon_h = \epsilon_-^\alpha + \epsilon_+^\alpha + \epsilon_-^\beta + \epsilon_+^\beta. \tag{3.30}$$

According to eq.(3.23), the variation yields

$$\begin{aligned} \mu &= M + \frac{\pi n}{2M_{\text{eff}}}, \\ T_\pm^f &= \frac{\pi n}{2M_{\text{eff}}} \mp \Lambda |c_1 + \sigma_f c_2|, \end{aligned} \tag{3.31}$$

and the total energy density is identified as

$$\begin{aligned} \epsilon &= \epsilon_0 + \epsilon_m + \epsilon_h \\ &= \epsilon_0 + 2\left(c_1^2 + c_2^2\right) + Mn + \frac{\pi n^2}{4M_{\text{eff}}} - \frac{1}{\pi} M_{\text{eff}} \Lambda^2 \left(c_1^2 + c_2^2\right). \end{aligned} \tag{3.32}$$

For $2\pi\rho_s > M_{\text{eff}}\Lambda^2$ the energy density has its minimum at

$$c_i = 0. \tag{3.33}$$

We again compare this result with eq.(3.6), the parameters c_i^3 still set to zero. Therefore, we still have $\cos\theta_0 = 0$ and $\theta_0 = \pm\frac{\pi}{2}$. Thus, each vector of the unit vector field $\vec{e}(x)$ points to the equator of the unit sphere, analogously to the two pocket-case. Moreover, $c_i = 0$ implies immediately that $k_i = 0$. Hence, unlike in the two pocket-case, in the four pocket-case no spiralization of the staggered magnetization occurs. This configuration is called homogeneous phase.

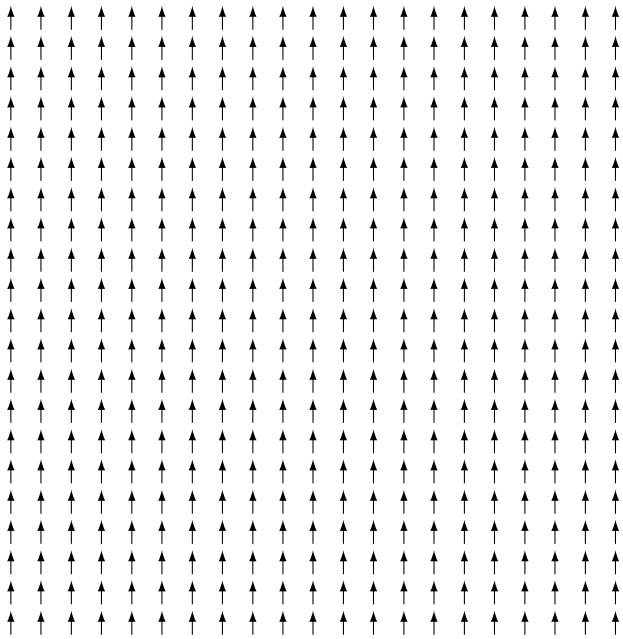

Figure 3.2: The homogeneous phase with a constant staggered magnetization.

Chapter 4

Investigation of a Piecewise Constant Potential

The calculations in section 3.3 were performed under the assumption of a constant potential c_1 in the x_1-direction, a constant potential c_2 in the x_2-direction, and of time-independent background fields such that $v_t = 0$. In both the two- and the four-pocket cases, at least one of the potentials c_i turned out to be zero. One may therefore wonder what happens if, on the one hand, the potential in one direction is set to zero beforehand, e.g. $c_2 = 0$, but on the other hand the system is given more degrees of freedom in the other direction x_1 by assuming the potential c_1 to have a periodic form consisting of several piecewise constant potentials where the lengths and the highs of the particular section adjust themselves. In the following chapter this idea is investigated more thoroughly by starting with the two pocket-case. We start with the two-pocket case because we have seen that, due to eq.(3.28), for two constant background potentials c_i a homogeneous spiral occurs in the staggered magnetization. Therefore, it is very likely that for this configuration the system makes use of the added degrees of freedom and adjusts itself in an interesting way. For the two-pocket case, we first consider a potential with two constant sections. The same principle is then applied to the two-pocket case with a potential consisting of three constant sections, which then allows us to extrapolate the obtained results for a case with k constant sections. In the second part of this chapter, we turn to the four-pocket case to find by means of analogous calculations the configuration chosen by the system in this case.

4.1 Two Filled Hole Pockets

In this section we deal with calculations of two pockets filled with holes. For that purpose, we obviously consider the pockets with the two lower energies E_-^α and E_-^β. In addition to that, we still restrict ourselves to time independent background field configurations, $v_t = 0$.

4.1.1 Two Sections

In our first investigation, the periodic potential is assumed to be split up in two constant parts c_{1a} and c_{1b} with the lengths L_a and L_b, respectively. The periodicity condition for such a potential reads

$$c_1(L_a + L_b + x) = c_1(x). \tag{4.1}$$

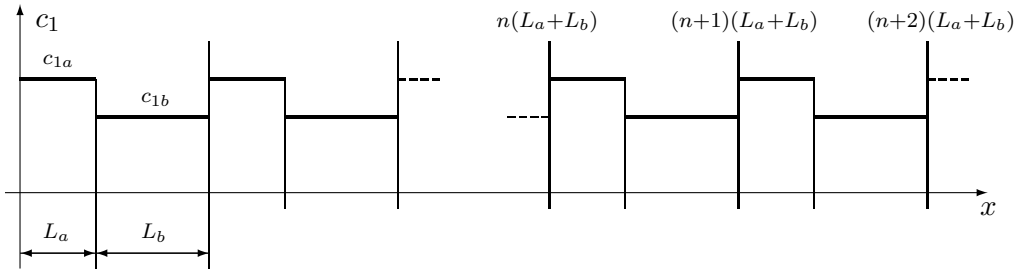

Figure 4.1: Periodic potential with two sections a and b. Each section $j \in \{a, b\}$ itself provides a constant potential c_{1j} with an corresponding length L_j.

Magnonic Contribution to the Energy

First, we consider the magnonic contribution to the energy density ϵ_m for this case. Generally, the magnonic energy is calculated as follows

$$\begin{aligned} E_m &= \int d^2x \ \frac{\rho_s}{2} \ \partial_i \vec{e} \cdot \partial_i \vec{e} \\ &= \int d^2x \ 2\rho_s \ v_i^+ v_i^-. \end{aligned} \tag{4.2}$$

The energy density for the magnonic contribution on condition that $v_t = 0$, $v_2^+ = v_2^- = c_2 = 0$, and $v_1^+ = v_1^- = c_1$ is thus calculated as

$$\begin{aligned} \epsilon_m &= \frac{1}{L_{x_1} L_{x_2}} \int_0^{L_{x_1}} dx_1 \int_0^{L_{x_2}} dx_2 \ 2\rho_s v_i^+ v_i^- \\ &= \frac{1}{N(L_a + L_b)} \int_0^{N(L_a+L_b)} dx_1 \ 2\rho_s c_1^2 \\ &= 2\rho_s \frac{1}{N(L_a + L_b)} \left(\int_0^{L_a} dx_1 \ c_{1a}^2 + \int_{L_a}^{L_a+L_b} dx_1 \ c_{1b}^2 + ... + \int_{(N-1)(L_a+L_b)+L_a}^{N(L_a+L_b)} dx_1 \ c_{1b}^2 \right) \\ &= 2\rho_s \frac{L_a c_{1a}^2 + L_b c_{1b}^2}{L_a + L_b}, \end{aligned} \tag{4.3}$$

with L_{x_1} and L_{x_2} denoting the lengths of a 2-dimensional box in the x_1- and the x_2-direction, respectively.

Fermionic Contribution to the Energy

The calculation of the fermionic contribution requires more effort and is shown in the following subsection. Under the premise of a periodic potential according to eq.(4.1), the displacement operator D acts on a field $\psi_\pm^f(x)$ as follows

$$^D\psi_\pm^f(x) = \psi_\pm^f(L_a + L_b + x) = e^{i(L_a+L_b)q} \psi_\pm^f(x), \tag{4.4}$$

where q denotes the Bloch momentum. The above operator D should not be confused with the operator D_i introduced earlier, which shifts one lattice space. According to eq.(3.14), the dispersion relation of the theory reads

$$E^f_{\pm}(p) = M + \frac{p_i^2}{2M'} + \sigma_f \frac{p_1 p_2}{M''} \pm \Lambda |c_1 - c_2|, \tag{4.5}$$

which, in the case of $c_2 = 0$ is reduced to

$$E^f_{\pm}(p) = M + \frac{p_i^2}{2M'} + \sigma_f \frac{p_1 p_2}{M''} \pm \Lambda c_1, \qquad c_1 \geq 0. \tag{4.6}$$

The corresponding eigenvectors are the following ones, respectively

$$\psi_{\pm}(x) = A e^{ip_1 x_1} e^{ip_2 x_2} \begin{pmatrix} \frac{1}{\sqrt{2}} \\ \pm\frac{1}{\sqrt{2}} \end{pmatrix}. \tag{4.7}$$

Let us now consider an ansatz for each interval $x \in [n(L_a + L_b), (n+1)(L_a + L_b)]$ separately. For notational convenience, we omit the flavor index f in the following considerations. In fact, for both flavors α and β, the calculation is the same. Thus, the flavor index will only reappear when the different flavors need to be taken into account as well. We also introduce two different momenta $p^{\pm}_{1j}$ to denote the forward momentum in the x_1-direction and the backward momentum in the $-x_1$-direction. If $x \in [(n-1)(L_a + L_b), (n-1)(L_a + L_b) + L_a]$, then

$$\psi_{a\pm}(x) = A_n e^{ip^+_{1a} x_1} e^{ip_2 x_2} \begin{pmatrix} \frac{1}{\sqrt{2}} \\ \pm\frac{1}{\sqrt{2}} \end{pmatrix} + B_n e^{ip^-_{1a} x_1} e^{ip_2 x_2} \begin{pmatrix} \frac{1}{\sqrt{2}} \\ \pm\frac{1}{\sqrt{2}} \end{pmatrix}, \tag{4.8}$$

and for $x \in [(n-1)(L_a + L_b) + L_a, n(L_a + L_b)]$

$$\psi_{b\pm}(x) = C_n e^{ip^+_{1b} x_1} e^{ip_2 x_2} \begin{pmatrix} \frac{1}{\sqrt{2}} \\ \pm\frac{1}{\sqrt{2}} \end{pmatrix} + D_n e^{ip^-_{1b} x_1} e^{ip_2 x_2} \begin{pmatrix} \frac{1}{\sqrt{2}} \\ \pm\frac{1}{\sqrt{2}} \end{pmatrix}. \tag{4.9}$$

Since the potential $c_1(x)$ is periodic, the Hamilton operator H commutes with the displacement operator D, and the eigenvectors of H can be chosen as the eigenvectors of D. Therefore, we end up with a standard quantum mechanical problem similar to the Kroenig-Penney model. First, consider $\psi_{a\pm}(x)$. By definition, we have for $x \in [n(L_a + L_b), (n+1)(L_a + L_b)]$

$$\begin{aligned} \psi_{a\pm}(x) &= A_n e^{ip^+_{1a}(x_1 - n(L_a+L_b))} e^{ip_2 x_2} \begin{pmatrix} \frac{1}{\sqrt{2}} \\ \pm\frac{1}{\sqrt{2}} \end{pmatrix} \\ &\quad + B_n e^{ip^-_{1a}(x_1 - n(L_a+L_b))} e^{ip_2 x_2} \begin{pmatrix} \frac{1}{\sqrt{2}} \\ \pm\frac{1}{\sqrt{2}} \end{pmatrix}, \end{aligned} \tag{4.10}$$

while for $x \in [(n+1)(L_a + L_b), (n+2)(L_a + L_b)]$

$$\begin{aligned} \psi_{a\pm}(x) &= A_{n+1} e^{ip^+_{1a}(x_1 - (n+1)(L_a+L_b))} e^{ip_2 x_2} \begin{pmatrix} \frac{1}{\sqrt{2}} \\ \pm\frac{1}{\sqrt{2}} \end{pmatrix} \\ &\quad + B_{n+1} e^{ip^-_{1a}(x_1 - (n+1)(L_a+L_b))} e^{ip_2 x_2} \begin{pmatrix} \frac{1}{\sqrt{2}} \\ \pm\frac{1}{\sqrt{2}} \end{pmatrix}. \end{aligned} \tag{4.11}$$

Performing a shift, we get

$$\begin{aligned}\psi_{a\pm}(x+L_a+L_b) &= A_{n+1}e^{ip_{1a}^{+}(x_1+L_a+L_b-(n+1)(L_a+L_b))}e^{ip_2x_2}\begin{pmatrix}\frac{1}{\sqrt{2}}\\ \pm\frac{1}{\sqrt{2}}\end{pmatrix}\\ &\quad +B_{n+1}e^{ip_{1a}^{-}(x_1+L_a+L_b-(n+1)(L_a+L_b))}e^{ip_2x_2}\begin{pmatrix}\frac{1}{\sqrt{2}}\\ \pm\frac{1}{\sqrt{2}}\end{pmatrix}\\ &= A_{n+1}e^{ip_{1a}^{+}(x_1-n(L_a+L_b))}e^{ip_2x_2}\begin{pmatrix}\frac{1}{\sqrt{2}}\\ \pm\frac{1}{\sqrt{2}}\end{pmatrix}\\ &\quad +B_{n+1}e^{ip_{1a}^{-}(x_1-n(L_a+L_b))}e^{ip_2x_2}\begin{pmatrix}\frac{1}{\sqrt{2}}\\ \pm\frac{1}{\sqrt{2}}\end{pmatrix}. \qquad (4.12)\end{aligned}$$

Considering eq.(4.4), this immediately leads to the conclusion that

$$A_{n+1}=A_ne^{i(L_a+L_b)q}, \qquad B_{n+1}=B_ne^{i(L_a+L_b)q}. \qquad (4.13)$$

The same operations hold for $\psi_{b\pm}(x)$ and yield

$$C_{n+1}=C_ne^{i(L_a+L_b)q}, \qquad D_{n+1}=D_ne^{i(L_a+L_b)q}. \qquad (4.14)$$

The conditions the hole field needs to fulfill are the continuity of $\psi(x)$ and the continuity of its first derivative $\psi'(x)$ at the junction of the potentials c_{1a} and c_{1b}. This leads to the following system of equations

$$\begin{aligned}\psi_{b\pm}\left((n+1)(L_a+L_b)\right) &= \psi_{a\pm}((n+1)(L_a+L_b)),\\ \psi_{a\pm}(n(L_a+L_b)+L_a) &= \psi_{b\pm}(n(L_a+L_b)+L_a),\\ \psi'_{b\pm}((n+1)(L_a+L_b)) &= \psi'_{a\pm}((n+1)(L_a+L_b)),\\ \psi'_{a\pm}(n(L_a+L_b)+L_a) &= \psi'_{b\pm}(n(L_a+L_b)+L_a). \qquad (4.15)\end{aligned}$$

The resulting system of linear equations can be expressed in matrix form as

$$U\ \vec{V}=\vec{0}, \qquad (4.16)$$

with

$$U=\begin{pmatrix} e^{i(L_a+L_b)q} & e^{i(L_a+L_b)q} & -e^{ip_{1b}^{+}(L_a+L_b)} & -e^{ip_{1b}^{-}(L_a+L_b)}\\ e^{ip_{1a}^{+}L_a} & e^{ip_{1a}^{-}L_a} & -e^{ip_{1b}^{+}L_a} & -e^{ip_{1b}^{-}L_a}\\ p_{1a}^{+}e^{i(L_a+L_b)q} & p_{1a}^{-}e^{i(L_a+L_b)q} & -p_{1b}^{+}e^{ip_{1b}^{+}(L_a+L_b)} & -p_{1b}^{-}e^{ip_{1b}^{-}(L_a+L_b)}\\ p_{1a}^{+}e^{ip_{1a}^{+}L_a} & p_{1a}^{-}e^{ip_{1a}^{-}L_a} & -p_{1b}^{+}e^{ip_{1b}^{+}L_a} & -p_{1b}^{-}e^{ip_{1b}^{-}L_a}\end{pmatrix}, \vec{V}=\begin{pmatrix}A_n\\ B_n\\ C_n\\ D_n\end{pmatrix}. \qquad (4.17)$$

We find non-trivial solutions of the system if we identify the roots of the determinant, $\det(U)=0$. The determinant reads

$$\begin{aligned}\det(U) &= e^{i(L_b(p_{1b}^{-}+q)+L_a(p_{1a}^{-}+p_{1b}^{-}+p_{1b}^{+}+q))}(p_{1b}^{-}-p_{1a}^{+})(p_{1a}^{-}-p_{1b}^{+})\\ &\quad -e^{i(L_b(p_{1b}^{-}+q)+L_a(p_{1a}^{+}+p_{1b}^{-}+p_{1b}^{+}+q))}(p_{1b}^{-}-p_{1a}^{-})(p_{1a}^{+}-p_{1b}^{+})\\ &\quad -e^{i(L_b(p_{1b}^{-}+p_{1b}^{+})+L_a(p_{1a}^{-}+p_{1a}^{+}+p_{1b}^{-}+p_{1b}^{+}))}(p_{1a}^{-}-p_{1a}^{+})(p_{1b}^{-}-p_{1b}^{+})\\ &\quad +e^{i(L_a(p_{1b}^{-}+p_{1b}^{+})+2(L_a+L_b)q)}(p_{1a}^{-}-p_{1a}^{+})(p_{1b}^{-}-p_{1b}^{+})\\ &\quad -e^{i(L_b(p_{1b}^{+}q)+L_a(p_{1a}^{+}+p_{1b}^{-}+p_{1b}^{+}+q))}(p_{1a}^{+}-p_{1b}^{-})(p_{1b}^{+}-p_{1a}^{-})\\ &\quad -e^{i(L_b(p_{1b}^{+}+q)+L_a(p_{1a}^{-}+p_{1b}^{-}+p_{1b}^{+}+q))}(p_{1a}^{-}-p_{1b}^{-})(p_{1b}^{+}-p_{1a}^{+}) \qquad (4.18)\end{aligned}$$

Since we are interested in finding a relation between the Bloch momentum q and the energy $E^f_\pm(q)$, we need to express the above determinant $\det(U)$ as a function of $E^f_\pm$. For the purpose of finding the lowest energy, we replace the different momenta $p^\pm_{1j}$ according to their dependence on the energy, considering only the lower energy term E^f_-. For $x \in [n(L_a+L_b), n(L_a+L_b)+L_a]$, we have the dispersion relation

$$E^f_-(p_{1a}, p_2) = M + \frac{p^2_{1a}+p^2_2}{2M'} + \sigma_f \frac{p_{1a}p_2}{M''} - \Lambda c_{1a}. \tag{4.19}$$

The above equation, solved for p_{1a}, leads to the momenta p^{f+}_{1a-} and p^{f-}_{1a-}

$$p^{f-}_{1a-} = \frac{-p_2\sigma_f M' - r^f_{1a-}}{M''}, \qquad p^{f+}_{1a-} = \frac{-p_2\sigma_f M' + r^f_{1a-}}{M''}, \tag{4.20}$$

where we use

$$r^f_{1j-} = \sqrt{p^2_2\,(M'^2 - M''^2) + 2M'M''^2(E^f_- - M + \Lambda c_{1j})}, \qquad j \in \{a, b\}. \tag{4.21}$$

Note that the plus and minus sign in the upper index denotes the forward and backward momentum, while the minus sign in the lower index refers to the lower energy E^f_-.

Of course, if we consider $x \in [n(L_a+L_b)+L_a, (n+1)(L_a+L_b)]$, we get analogously the same results, this time with the relevant potential c_{1b}

$$p^{f-}_{1b-} = \frac{-p_2\sigma_f M' - r^f_{1b-}}{M''}, \qquad p^{f+}_{1b-} = \frac{-p_2\sigma_f M' + r^f_{1b-}}{M''}. \tag{4.22}$$

Plugging the above eqns.(4.20) and (4.22) in eq.(4.18), we get the following form for the determinant $\det(U)$

$$\begin{aligned}
\det(U) \;=\; & \frac{1}{2M''^2}\Bigg\{ 8e^{i\left[(L_a+L_b)q - \frac{(3L_a+L_b)p_2\sigma_f M'}{M''}\right]} \\
& \left[2r^f_{1a-}r^f_{1b-}\left[\cos\left(\frac{L_a r^f_{1a-}}{M''}\right)\cos\left(\frac{L_b r^f_{1b-}}{M''}\right) - \cos\left(\frac{(L_a+L_b)\,(M''q + M'p_2\sigma_f)}{M''}\right)\right]\right. \\
& \left. - \sin\left(\frac{L_a r^f_{1a-}}{M''}\right)\sin\left(\frac{L_b r^f_{1b-}}{M''}\right)\left((r^f_{1a-})^2 + (r^f_{1b-})^2\right)\right]\Bigg\}
\end{aligned} \tag{4.23}$$

Since we are interested in the roots of $\det(U)$, we simplify this equation by omitting the non-relevant factors and writing it in the following form

$$\begin{aligned}
0 \;=\; & 2\cos\left(\frac{L_a r^f_{1a-}}{M''}\right)\cos\left(\frac{L_b r^f_{1b-}}{M''}\right) - 2\cos\left(\frac{(L_a+L_b)\,(M''q + M'p_2\sigma_f)}{M''}\right) \\
& - \frac{\sin\left(\frac{L_a r^f_{1a-}}{M''}\right)\sin\left(\frac{L_b r^f_{1b-}}{M''}\right)\left((r^f_{1a-})^2 + (r^f_{1b-})^2\right)}{r^f_{1a-}r^f_{1b-}}.
\end{aligned} \tag{4.24}$$

We call this truncated function $f_-^f(E_-^f, q, p_2)$

$$\begin{aligned} f_-^f(E_-^f, q, p_2) &= 2\cos\left(\frac{L_a r_{1a-}^f}{M''}\right)\cos\left(\frac{L_b r_{1b-}^f}{M''}\right) - 2\cos\left(\frac{(L_a+L_b)\,(M''q + M' p_2 \sigma_f)}{M''}\right) \\ &\quad - \frac{\sin\left(\frac{L_a r_{1a-}^f}{M''}\right)\sin\left(\frac{L_b r_{1b-}^f}{M''}\right)\left((r_{1a-}^f)^2 + (r_{1b-}^f)^2\right)}{r_{1a-}^f r_{1b-}^f}. \end{aligned} \tag{4.25}$$

At this point, we still want to find an explicit expression for E_-^f. However, the relation

$$f_-^f(E_-^f, q, p_2) = 0 \tag{4.26}$$

is still not analytically solvable for E_-^f. If we dope the material with a small density of holes, we are allowed to expand $f_-^f(E_-^f, q, p_2)$ around the lowest energy residing at $q = 0$ and $p_2 = 0$ up to $\mathcal{O}(p^2)$,

$$\begin{aligned} f_-^f(E_-^f, q, p_2) &= f_-^f(E_-^f, 0, 0) + \frac{1}{2}\frac{\partial^2}{\partial q^2} f_-^f(E_-^f, 0, 0) q^2 \\ &\quad + \frac{1}{2}\frac{\partial^2}{\partial p_2^2} f_-^f(E_-^f, 0, 0) p_2^2 + \frac{\partial^2}{\partial q\, \partial p_2} f_-^f(E_-^f, 0, 0) q p_2. \end{aligned} \tag{4.27}$$

Note that there are no first order terms in this expansion. The surface of the function f_-^f for a fixed energy E_-^f thus describes an ellipse, just as expected due to the hole pockets, which are indeed elliptically shaped. For further simplification, we linearize the energy $E_-^f(q, p_2)$ as well, expanding it around its minimum at $q = 0$ and $p_2 = 0$ up to order $\mathcal{O}(\delta E_-^f) \sim \mathcal{O}(p^2)$

$$E_-^f(q, p_2) = E_-^f(0, 0) + \delta E_-^f(q, p_2). \tag{4.28}$$

Denoting $E_-^f(0, 0) = E_-^0$ (comparing with eq.(4.6), we find that $E_-^\alpha(0, 0) = E_-^\beta(0, 0) = E_-^0$), we linearize

$$f_-^f(E_-^f, 0, 0) = f_-^f(E_-^0, 0, 0) + \frac{\partial}{\partial E_-^f} f_-^f(E_-^0, 0, 0)\ \delta E_-^f(q, p_2), \tag{4.29}$$

and get the final form of the expansion which reads

$$\begin{aligned} f_-^f(E_-^f, q, p_2) &= \frac{\partial}{\partial E_-^f} f_-^f(E_-^0, 0, 0)\ \delta E_-^f(q, p_2) + \frac{1}{2}\frac{\partial^2}{\partial q^2} f_-^f(E_-^0, 0, 0) q^2 \\ &\quad + \frac{1}{2}\frac{\partial^2}{\partial p_2^2} f_-^f(E_-^0, 0, 0) p_2^2 + \frac{\partial^2}{\partial q\, \partial p_2} f_-^f(E_-^0, 0, 0) q p_2. \end{aligned} \tag{4.30}$$

Consider now a Fermi surface with $E(q, p_2) = E^0 + \delta E(q, p_2) = \text{const}$ and denote the kinetic energy T_-^f as

$$T_-^f = \delta E_-^f(q, p_2) = E_-^f(q, p_2) - E_-^0. \tag{4.31}$$

Using eq.(4.26) and eq.(4.30), we identify

$$T_-^f = \delta E_-^f(q, p_2) = -\left(\frac{\partial f_-^f}{\partial E_-^f}\right)^{-1}\left(\frac{1}{2}\frac{\partial^2 f_-^f}{\partial q^2} q^2 + \frac{1}{2}\frac{\partial^2 f_-^f}{\partial q_2^2} p_2^2 + \frac{\partial^2 f_-^f}{\partial q \partial p_2} q p_2\right). \tag{4.32}$$

The fermion density n_-^f is calculated according to eq.(3.16). We find

$$n_-^f = \frac{1}{(2\pi)^2}\int_{P_-^f} dp_2\ dq = \frac{1}{4\pi}F_-^f T_-^f, \tag{4.33}$$

where we denote

$$F_-^f = \frac{2\left(\frac{\partial f_-^f}{\partial E_-^f}\right)}{\sqrt{\left(\frac{\partial^2 f_-^f}{\partial q^2}\right)\left(\frac{\partial^2 f_-^f}{\partial p_2^2}\right) - \left(\frac{\partial^2 f_-^f}{\partial q\ \partial p_2}\right)^2}}. \tag{4.34}$$

The kinetic energy density t_-^f of an occupied hole-pocket is calculated according to eq.(3.18). Adapting this calculation to our case, we find

$$t_-^f = \frac{1}{(2\pi)^2}\int_{P_-^f} dp_2\ dq\ T_-^f = \frac{1}{8\pi}F_-^f {T_-^f}^2. \tag{4.35}$$

The total energy density of one hole is given by

$$\epsilon_-^f = E_-^0 n_-^f + t_-^f, \tag{4.36}$$

which gives us the total energy density ϵ_h of the two holes

$$\epsilon_h = \epsilon_-^\alpha + \epsilon_-^\beta. \tag{4.37}$$

The filling of the two hole-pockets depends on the parameters T_-^f, which we vary to minimize the energy. We proceed exactly as suggested in section 3.2.2. To solve the variational problem, we again introduce eq.(3.22) with a Lagrange multiplier μ allowing us to keep the hole density n fixed.

$$S = \epsilon_h - \mu n \tag{4.38}$$

The variational problem demands

$$\frac{\partial S}{\partial T_-^f} = 0. \tag{4.39}$$

Since we have

$$\begin{aligned}\frac{\partial S}{\partial T_-^f} &= \frac{\partial}{\partial T_-^f}\left(E_-^0(n_-^\alpha + n_-^\beta) + t_-^\alpha + t_-^\beta - \mu(n_-^\alpha + n_-^\beta)\right)\\ &= \frac{1}{4\pi}F_-^f\left(E_-^0 - \mu + T_-^f\right)\\ &\stackrel{!}{=} 0,\end{aligned} \tag{4.40}$$

we identify the relevant parameters

$$\begin{aligned}\mu &= \frac{4\pi}{F_-^\alpha + F_-^\beta}n + E_-^0,\\ T_-^f &= \frac{4\pi}{F_-^\alpha + F_-^\beta}n.\end{aligned} \tag{4.41}$$

Considering this derivation of the fermionic contribution ϵ_h as well the previously discussed magnonic contribution ϵ_m as derived in eq.(4.3), the total energy density consequently reads

$$\epsilon = \epsilon_0 + 2\rho_s\frac{L_a c_{1a}^2 + L_b c_{1b}^2}{L_a + L_b} + E_-^0 n + \frac{2\pi}{F_-^\alpha + F_-^\beta}n^2. \tag{4.42}$$

Calculation of the Background Field Configuration

To calculate the above total energy density, we still lack E_-^0. Comparing with eq.(3.28), we recognize the linearity of the potentials c_i in n. Since we are still working with small hole densities n, we are allowed to expand the potentials c_{1j} in n as well

$$c_{1j} = \gamma_{1j} n + \mathcal{O}(n^2), \qquad j \in \{a, b\}, \qquad \gamma_{1j} \in \mathbb{R}. \tag{4.43}$$

We thus rewrite the implicit equation eq.(4.24) for E_-^0 as a first order approximation of the potentials c_{1j} in n

$$\begin{aligned} -1 + \cos\left((L_a + L_b)\sqrt{2M'(E_-^0 - M)}\right) = \\ \frac{M'\left(L_a\gamma_{1a} + L_b\gamma_{1b}\right)\Lambda \sin\left((L_a + L_b)\sqrt{2M'(E_-^0 - M)}\right)}{\sqrt{2M'(E_-^0 - M)}} n. \end{aligned} \tag{4.44}$$

This equation is still not analytically solvable for E_-^0. However, according to eq.(4.6), E_-^0 is linear in c_1. Therefore, we also linearize $E_-^0 = M + \Delta n$ with a yet unknown correction Δn. Eq.(4.44) can then be rewritten as

$$-1 + \cos\left((L_a + L_b)\sqrt{2M'\Delta n}\right) = \frac{M'\left(L_a\gamma_{1a} + L_b\gamma_{1b}\right)\Lambda \sin\left((L_a + L_b)\sqrt{2M'\Delta n}\right)}{\sqrt{2M'\Delta n}} n. \tag{4.45}$$

The total energy density ϵ is calculated up to $\mathcal{O}(n^2)$. Since the energy E_-^0 appears in the linear term of the energy density already, we only need to consider the correction Δn to be of order n. A short calculation yields the approximation up to order $\mathcal{O}\left((\sqrt{\Delta n})^2\right) \sim \mathcal{O}(n)$,

$$\Delta n = -\frac{\left(L_a\gamma_{1a} + L_b\gamma_{1b}\right)\Lambda}{L_a + L_b} n. \tag{4.46}$$

Thus, the energy E_-^0 written in first order approximation reads

$$E_-^0 = M - \frac{\left(L_a\gamma_{1a} + L_b\gamma_{1b}\right)\Lambda}{L_a + L_b} n, \tag{4.47}$$

which gives us the energy density up to order $\mathcal{O}(n^2)$

$$\epsilon = \epsilon_0 + Mn + \left(\frac{2\rho_s(L_a\gamma_{1a}^2 + L_b\gamma_{1b}^2) - \Lambda(L_a\gamma_{1a} + L_b\gamma_{1b})}{L_a + L_b} + \frac{\pi}{2M_{\text{eff}}}\right) n^2. \tag{4.48}$$

We are now interested in how this particular system adjusts itself by minimizing the energy density ϵ. Therefore, ϵ needs to be varied with respect to both potentials γ_{1j} as well as with respect to both lengths L_j, such that

$$\frac{\partial \epsilon}{\partial L_j} = \frac{\partial \epsilon}{\partial \gamma_{1j}} = 0. \tag{4.49}$$

Solving this system of equations yields the result

$$\gamma_{1a} = \gamma_{1b} = \frac{\Lambda}{4\rho_s}, \tag{4.50}$$

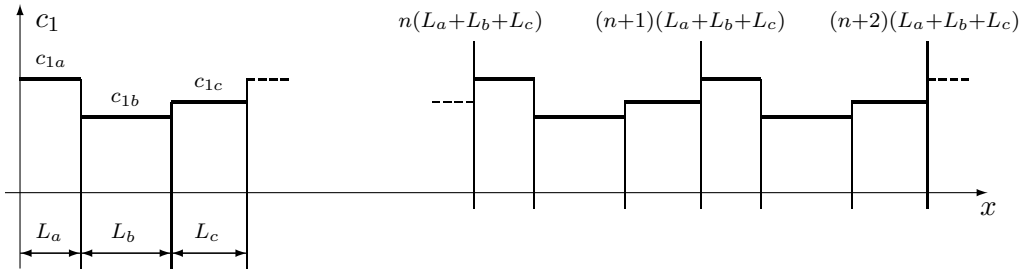

Figure 4.2: Periodic potential with three sections a, b and c. Each section $i \in \{a, b, c\}$ itself provides a constant potential c_{1i} with a corresponding length L_i.

and thus

$$c_{1a} = c_{1b} = \frac{\Lambda}{4\rho_s} n. \tag{4.51}$$

The case for two potentials therefore reproduces the result for a single constant potential c_1, causing a homogeneous zero degree spiral as previously seen in section (3.28).

4.1.2 Three Sections

The two potential case as discussed in section 4.1.1 did not lead to a new background field configuration with an inhomogeneous spiralization of the staggered magnetization. We therefore ask ourselves what happens if the system is given more freedom. Again, the potential in the x_1-direction is assumed to have a periodic form. Only this time, we add one more division c to the periodic configuration. In this case, we have a periodic background field with three constant parts c_{1a}, c_{1b}, and c_{1c} with the lengths L_a, L_b, and L_c, respectively. For the calculation, we proceed as we did for the case of two potentials. To keep the notation as simple as possible, we omit the use of indices referring to the three-potential case in this section. Therefore, if not specified otherwise, variables used before now are linked to the three potential case. The periodicity condition for the potential $c_1(x)$ reads

$$c_1(L_a + L_b + L_c + x) = c_1(x). \tag{4.52}$$

Magnonic Contribution to the Energy

The magnonic contribution to the energy is calculated analogously to subsection 4.1.1. In the three-potential case, we identify the energy density ϵ_m as

$$\epsilon_m = 2\rho_s \frac{L_a c_{1a}^2 + L_b c_{1b}^2 + L_c c_{1c}^2}{L_a + L_b + L_c}. \tag{4.53}$$

Since we apply the same concept as in the case of two potentials, this calculation is still based on the assumption that $v_t = 0$, $v_2^+ = v_2^- = c_2 = 0$, and $v_1^+ = v_1^- = c_1$.

Fermionic Contribution to the Energy

The fermionic contribution in the three-potential case is derived analogously to the two-potential case as well. However, some adjustments have to be made. The displacement operator D acts on a field $\psi^f_\pm(x)$ as

$$^D\psi^f_\pm(x) = \psi^f_\pm(L_a + L_b + L_c + x) = e^{i(L_a+L_b+L_c)q}\psi^f_\pm(x), \tag{4.54}$$

with q denoting the Bloch momentum. The dispersion relation for a hole of flavor f, still under the premise that $c_2 = 0$, remains the same as for the two potential case (see eq.(4.6)). Therefore, we also have the eigenvectors according to eq.(4.7). For notational convenience, we again omit the flavor index f in the following calculation. It will reappear when it is necessary to do so.

For the hole field $\psi(x)_\pm$, we again make an ansatz for each section separately. If $x \in [(n-1)(L_a + L_b + L_c), (n-1)(L_a + L_b + L_c) + L_a]$, then

$$\psi_{a\pm}(x) = A_n e^{ip^+_{1a}x_1}e^{ip_2x_2}\begin{pmatrix} \frac{1}{\sqrt{2}} \\ \pm\frac{1}{\sqrt{2}} \end{pmatrix} + B_n e^{ip^-_{1a}x_1}e^{ip_2x_2}\begin{pmatrix} \frac{1}{\sqrt{2}} \\ \pm\frac{1}{\sqrt{2}} \end{pmatrix}. \tag{4.55}$$

For $x \in [(n-1)(L_a + L_b + L_c) + L_a, (n-1)(L_a + L_b + L_c) + L_a + L_b]$,

$$\psi_{b\pm}(x) = C_n e^{ip^+_{1b}x_1}e^{ip_2x_2}\begin{pmatrix} \frac{1}{\sqrt{2}} \\ \pm\frac{1}{\sqrt{2}} \end{pmatrix} + D_n e^{ip^-_{1b}x_1}e^{ip_2x_2}\begin{pmatrix} \frac{1}{\sqrt{2}} \\ \pm\frac{1}{\sqrt{2}} \end{pmatrix}, \tag{4.56}$$

and finally if $x \in [(n-1)(L_a + L_b + L_c) + L_a + L_b, n(L_a + L_b + L_c)]$,

$$\psi_{c\pm}(x) = E_n e^{ip^+_{1c}x_1}e^{ip_2x_2}\begin{pmatrix} \frac{1}{\sqrt{2}} \\ \pm\frac{1}{\sqrt{2}} \end{pmatrix} + F_n e^{ip^-_{1c}x_1}e^{ip_2x_2}\begin{pmatrix} \frac{1}{\sqrt{2}} \\ \pm\frac{1}{\sqrt{2}} \end{pmatrix}. \tag{4.57}$$

Due to the properties of the displacement operator D, the coefficients of the hole field are related as

$$\begin{aligned} A_{n+1} &= A_n e^{i(L_a+L_b+L_c)q}, & B_{n+1} &= B_n e^{i(L_a+L_b+L_c)q}, \\ C_{n+1} &= C_n e^{i(L_a+L_b+L_c)q}, & D_{n+1} &= D_n e^{i(L_a+L_b+L_c)q}, \\ E_{n+1} &= E_n e^{i(L_a+L_b+L_c)q}, & F_{n+1} &= F_n e^{i(L_a+L_b+L_c)q}. \end{aligned} \tag{4.58}$$

We consider the continuity of the hole field $\psi(x)$ and its first derivative $\psi'(x)$ and modify the set of equations we established in eq.(4.15) in order to describe the three potential case.

$$\begin{aligned} \psi_{a\pm}\left((n+1)(L_a + L_b + L_c)\right) &= \psi_{c\pm}((n+1)(L_a + L_b + L_c)), \\ \psi_{b\pm}(n(L_a + L_b + L_c) + L_a + L_b) &= \psi_{c\pm}(n(L_a + L_b + L_c) + L_a + L_c), \\ \psi_{a\pm}(n(L_a + L_b + L_c) + L_a) &= \psi_{b\pm}(n(L_a + L_b + L_c) + L_a), \\ \psi'_{a\pm}\left((n+1)(L_a + L_b + L_c)\right) &= \psi'_{c\pm}((n+1)(L_a + L_b + L_c)), \\ \psi'_{b\pm}(n(L_a + L_b + L_c) + L_a + L_b) &= \psi'_{c\pm}(n(L_a + L_b + L_c) + L_a + L_c), \\ \psi'_{a\pm}(n(L_a + L_b + L_c) + L_a) &= \psi'_{b\pm}(n(L_a + L_b + L_c) + L_a). \end{aligned} \tag{4.59}$$

The system of linear equations expressed in matrix form reads

$$U\ \vec{V} = \vec{0}, \tag{4.60}$$

with

$$U = \begin{pmatrix}
e^{i(L_a+L_b+L_c)q} & e^{i(L_a+L_b+L_c)q} & 0 & 0 & -e^{ip_{1c}^{+}(L_a+L_b+L_c)} & -e^{ip_{1c}^{-}(L_a+L_b+L_c)} \\
e^{ip_{1a}^{+}L_a} & e^{ip_{1a}^{-}L_a} & -e^{ip_{1b}^{+}L_a} & -e^{ip_{1b}^{-}L_a} & 0 & 0 \\
0 & 0 & e^{ip_{1b}^{+}(L_a+L_b)} & e^{ip_{1b}^{-}(L_a+L_b)} & -e^{ip_{1c}^{+}(L_a+L_b)} & -e^{ip_{1c}^{-}(L_a+L_b)} \\
p_{1a}^{+}e^{ip_{1a}^{+}L_a} & p_{1a}^{-}e^{ip_{1a}^{-}L_a} & -p_{1b}^{+}e^{ip_{1b}^{+}L_a} & -p_{1b}^{-}e^{ip_{1b}^{+}L_a} & 0 & 0 \\
p_{1a}^{+}e^{i(L_a+L_b+L_c)q} & p_{1a}^{-}e^{i(L_a+L_b+L_c)q} & 0 & 0 & -p_{1c}^{+}e^{ip_{1c}^{+}(L_a+L_b+L_c)} & -p_{1c}^{-}e^{ip_{1c}^{-}(L_a+L_b+L_c)} \\
0 & 0 & p_{1b}^{+}e^{ip_{1b}^{+}(L_a+L_b)} & p_{1b}^{-}e^{ip_{1b}^{-}(L_a+L_b)} & -p_{1c}^{+}e^{ip_{1c}^{+}(L_a+L_b)} & -p_{1c}^{-}e^{ip_{1c}^{-}(L_a+L_b)}
\end{pmatrix} \tag{4.61}$$

and

$$\vec{V}^T = (A_n, B_n, C_n, D_n, E_n, F_n). \tag{4.62}$$

Again, we look for the non-trivial solutions of this system by finding the roots of the determinant $\det(U) = 0$. After substituting the momenta $p_{1j}^{f\pm}$ according to the dispersion relation for the lower energy E_-^f in eq.(4.6)

$$p_{1j-}^{f\pm} = \frac{-p_2\sigma_f M' \pm r_{1j-}^f}{M''}, \qquad j \in \{a, b, c\}, \tag{4.63}$$

and omitting the non-relevant factors, the equation $\det(U) = 0$ is replaced by the equation

$$f_-^f(E_-^f, q, p_2) = 0, \tag{4.64}$$

where

$$\begin{aligned}
&f_-^f(E_-^f, q, p_2) = \\
&2\cos\left(\frac{(L_a+L_b+L_c)\,(M''q + M'p_2\sigma_f)}{M''}\right) - 2\cos\left(\frac{L_a r_{1a-}^f}{M''}\right)\cos\left(\frac{L_b r_{1b-}^f}{M''}\right)\cos\left(\frac{L_c r_{1c-}^f}{M''}\right) \\
&\quad + \frac{\sin\left(\frac{L_a r_{1a-}^f}{M''}\right)\sin\left(\frac{L_b r_{1b-}^f}{M''}\right)\cos\left(\frac{L_c r_{1c-}^f}{M''}\right)\left((r_{1a-}^f)^2 + (r_{1b-}^f)^2\right)}{r_{1a-}^f r_{1b-}^f} \\
&\quad + \frac{\sin\left(\frac{L_a r_{1a-}^f}{M''}\right)\cos\left(\frac{L_b r_{1b-}^f}{M''}\right)\sin\left(\frac{L_c r_{1c-}^f}{M''}\right)\left((r_{1a-}^f)^2 + (r_{1c-}^f)^2\right)}{r_{1a-}^f r_{1c-}^f} \\
&\quad + \frac{\cos\left(\frac{L_a r_{1a-}^f}{M''}\right)\sin\left(\frac{L_b r_{1b-}^f}{M''}\right)\sin\left(\frac{L_c r_{1c-}^f}{M''}\right)\left((r_{1b-}^f)^2 + (r_{1c-}^f)^2\right)}{r_{1b-}^f r_{1c-}^f}.
\end{aligned} \tag{4.65}$$

We then expand the function $f_-^f(E_-^f, q, p_2)$ around the lowest energy residing at $q = 0$ and $p_2 = 0$ according to eq.(4.27) up to $\mathcal{O}(p^2)$. The coefficients of the expansion are listed in the appendix. Proceeding exactly as in the two-potential case shown in subsection 4.1.1, the

total energy density up to $\mathcal{O}(n^2)$ is identified in the three-potential case in a straightforward manner as

$$\epsilon = \epsilon_0 + 2\rho_s \frac{L_a c_{1a}^2 + L_b c_{1b}^2 + L_c c_{1c}^2}{L_a + L_b + L_c} + E_-^0 n + \frac{2\pi}{F_-^\alpha + F_-^\beta} n^2. \tag{4.66}$$

Calculation of the Background Field Configuration

To calculate the energy density for three potentials, eq.(4.66), we again proceed analogously to the two-potential case shown in subsection 4.1.1. We expand the potentials c_{1j} according to eq.(4.43)

$$c_{1j} = \gamma_{1j} n + \mathcal{O}(n^2), \qquad j \in \{a, b, c\}, \qquad \gamma_{1j} \in \mathbb{R}. \tag{4.67}$$

In addition, we also linearize the minimal energy $E_-^0 = M + \Delta n$. Plugging these two approximations into eq.(4.64), the correction Δn for the energy up to order $\mathcal{O}((\sqrt{\Delta n})^2)$ yields

$$\Delta n = -\frac{(L_a \gamma_{1a} + L_b \gamma_{1b} + L_c \gamma_{1c})\,\Lambda}{L_a + L_b + L_c} n \tag{4.68}$$

and thus

$$E_-^0 = M - \frac{(L_a \gamma_{1a} + L_b \gamma_{1b} + L_c \gamma_{1c})\,\Lambda}{L_a + L_b + L_c} n. \tag{4.69}$$

The energy density for the three-potential case up to $\mathcal{O}(n^2)$ then reads

$$\epsilon = \epsilon_0 + Mn + \left(\frac{2\rho_s (L_a \gamma_{1a}^2 + L_b \gamma_{1b}^2 + L_c \gamma_{1c}^2) - \Lambda (L_a \gamma_{1a} + L_b \gamma_{1b} + L_c \gamma_{1c})}{L_a + L_b + L_c} + \frac{\pi}{2M_{\text{eff}}} \right) n^2. \tag{4.70}$$

The variation of the energy density according to eq.(4.49) gives

$$\gamma_{1a} = \gamma_{1b} = \gamma_{1c} = \frac{\Lambda}{4\rho_s}, \tag{4.71}$$

and thus

$$c_{1a} = c_{1b} = c_{1c} = \frac{\Lambda}{4\rho_s} n. \tag{4.72}$$

Obviously, the three-potential case again reproduces the result we have obtained previously for a single constant potential c_1 in eq.(3.28) and for two potentials c_{1a} and c_{1b} in eq.(4.51), causing again a homogeneous zero-degree spiral.

4.1.3 Extrapolation for k Sections

The explicit execution for the two-section case and the three-section case raises the question of a general form for the problem. At this point, we lack a mathematical proof for the k-section case. Nonetheless, due to locality considerations of the problem, there is little doubt that each added potential c_{1j} and the according length L_j will enter in a totally symmetric way into the problem. The general form for the energy density ϵ is hence expected to read

$$\epsilon = \epsilon_0 + Mn + \left(\frac{2\rho_s \sum_j L_j \gamma_{1j}^2 - \Lambda \sum_j L_j \gamma_{1j}}{\sum_j L_j} + \frac{\pi}{2M_{\text{eff}}} \right) n^2. \tag{4.73}$$

For an arbitrarily large number of sections the variation of the energy according to eq.(4.49) then yields

$$\gamma_{1a} = \gamma_{1b} = ... = \gamma_{1k} = \frac{\Lambda}{4\rho_s}, \tag{4.74}$$

and thus

$$c_{1a} = c_{1b} = ... = c_{1k} = \frac{\Lambda}{4\rho_s} n. \tag{4.75}$$

Hence, even for an arbitrarily large number of sections the system establishes a constant background potential causing a zero-degree spiral. Since we can approximate any continuous periodic background potential with this model, we conclude that for small doping the constant background potential remains the energetically most favorable configuration and within the range of $1 < \frac{\Lambda^2 M_{\text{eff}}}{2\rho_s \pi} < 2$, the system always establishes a zero-degree spiral.

4.2 Four Filled Hole Pockets

In this section, we perform the same calculations as we did for the two-pocket case, only this time slightly modified for four filled hole pockets. We thus take into account all energies $E^f_\pm$ and, as we have done throughout this work, we only consider time-independent background fields $v_t = 0$.

4.2.1 Two Sections

We again start by considering the background potential with two constant sections introduced in subsection 4.1.1 with the periodicity condition eq.(4.1) leading to a background field as shown in figure 4.1.1. The calculation for the four-pocket case is then performed analogously to the two-pocket case with some minor adjustments.

Magnonic Contribution to the Energy

The magnonic contribution to the energy density does not depend on the number of filled hole pockets. In the two-section calculation for four filled hole pockets, we therefore have the magnonic energy density as calculated in eq.(4.3)

$$\epsilon_m = 2\rho_s \frac{L_a c_{1a}^2 + L_b c_{1b}^2}{L_a + L_b}. \tag{4.76}$$

Fermionic Contribution to the Energy

The calculation of the fermionic contribution to the energy can also be performed analogously to section 4.1.1. However, this time we need to consider the dispersion relation for both the upper and the lower energy level

$$E^f_\pm(p_{1j}, p_2) = M + \frac{p_{1j}^2 + p_2^2}{2M'} + \sigma_f \frac{p_{1j}^2}{M''} \pm \Lambda c_{1j}. \tag{4.77}$$

This equation, solved for each section individually, leads to the forward momentum $p^{f+}_{1j\pm}$ and the backward momentum $p^{f-}_{1j\pm}$ as

$$p^{f+}_{1j\pm} = \frac{-p_s \sigma_f M' + r^f_{1j\pm}}{M''}, \qquad p^{f-}_{1j\pm} = \frac{-p_s \sigma_f M' - r^f_{1j\pm}}{M''}, \tag{4.78}$$

where we use again

$$r^f_{1j\pm} = \sqrt{p_2^2(M'^2 - M''^2) + 2M'M''^2(E^f_\pm - M \mp \Lambda c_{1j})}, \qquad j \in \{a, b\}. \tag{4.79}$$

Note again that a plus- or minus-sign in the upper index refers to the forward or backward momentum, while a plus- or minus-sign in the lower index refers to the higher or the lower energy level, respectively.

Since we deal with the two section potential, we still need the hole field to fulfill the conditions proposed in eq.(4.15). The procedure to solve that problem is analogous to the two-pocket case which leads to the function $f^f_\pm(E^f_\pm, q, p_2)$

$$\begin{aligned} f^f_\pm(E^f_\pm, q, p_2) \;=\; & 2\cos\left(\frac{L_a r^f_{1a\pm}}{M''}\right)\cos\left(\frac{L_b r^f_{1b\pm}}{M''}\right) - 2\cos\left(\frac{(L_a + L_b)\,(M''q + M'p_2\sigma_f)}{M''}\right) \\ & - \frac{\sin\left(\frac{L_a r^f_{1a\pm}}{M''}\right)\sin\left(\frac{L_b r^f_{1b\pm}}{M''}\right)\left((r^f_{1a\pm})^2 + (r^f_{1b\pm})^2\right)}{r^f_{1a\pm} r^f_{1b\pm}}. \end{aligned} \tag{4.80}$$

Considering a Fermi surface with $E^f_\pm(q, p_2) = E^0_\pm + \delta E^f_\pm(q, p_2) = \text{const}$ and denoting the kinetic energy $T^f_\pm$ as

$$T^f_\pm = \delta E^f_\pm(q, p_2) = E^f_\pm(q, p_2) - E^0_\pm, \tag{4.81}$$

we find the fermion density $n^f_\pm$ analogously to eq.(4.33)

$$n^f_\pm = \frac{1}{(2\pi)^2}\int_{P^f_\pm} dp_2\; dq = \frac{1}{4\pi} F^f_\pm T^f_\pm, \tag{4.82}$$

where we denote

$$F^f_\pm = \frac{2\left(\frac{\partial f^f_\pm}{\partial E^f_\pm}\right)}{\sqrt{\left(\frac{\partial^2 f^f_\pm}{\partial q^2}\right)\left(\frac{\partial^2 f^f_\pm}{\partial p_2^2}\right) - \left(\frac{\partial^2 f^f_\pm}{\partial q\;\partial p_2}\right)^2}}. \tag{4.83}$$

The kinetic energy density $t^f_\pm$ of an occupied hole pocket is calculated as proposed in eq.(4.35)

$$t^f_\pm = \frac{1}{(2\pi)^2}\int_{P^f_\pm} dp_2\; dq\; T^f_\pm = \frac{1}{8\pi} F^f_\pm {T^f_\pm}^2. \tag{4.84}$$

The total energy density of one hole is given by

$$\epsilon^f_\pm = E^0_\pm n^f_\pm + t^f_\pm, \tag{4.85}$$

which is then used to calculate the total energy density ϵ_h of the four holes

$$\epsilon_h = \epsilon^\alpha_- + \epsilon^\alpha_+ + \epsilon^\beta_- + \epsilon^\beta_+. \tag{4.86}$$

Fixing the hole density n by introducing a Lagrange multiplier μ according to eq.(4.38) such that

$$S = \epsilon_h - \mu n \tag{4.87}$$

and solving the variational problem

$$\frac{\partial S}{\partial T_{\pm}^{f}} = 0 \tag{4.88}$$

leads to the parameters

$$\begin{aligned}
\mu &= \frac{4\pi n + E_{-}^{0}\left(F_{-}^{\alpha}+F_{-}^{\beta}\right) + E_{+}^{0}\left(F_{+}^{\alpha}+F_{+}^{\beta}\right)}{F_{-}^{\alpha}+F_{+}^{\alpha}+F_{-}^{\beta}+F_{+}^{\beta}}, \\
T_{+}^{f} &= \frac{4\pi n - E_{-}^{0}\left(F_{-}^{\alpha}+F_{-}^{\beta}\right) + E_{+}^{0}\left(F_{-}^{\alpha}+F_{-}^{\beta}\right)}{F_{-}^{\alpha}+F_{+}^{\alpha}+F_{-}^{\beta}+F_{+}^{\beta}}, \\
T_{-}^{f} &= \frac{4\pi n + E_{-}^{0}\left(F_{+}^{\alpha}+F_{+}^{\beta}\right) - E_{+}^{0}\left(F_{+}^{\alpha}+F_{+}^{\beta}\right)}{F_{-}^{\alpha}+F_{+}^{\alpha}+F_{-}^{\beta}+F_{+}^{\beta}}.
\end{aligned} \tag{4.89}$$

Together with eq.(4.76), we can thus express the total energy density

$$\begin{aligned}
\epsilon &= \epsilon_0 + 2\rho_s \frac{L_a^2 c_{1a}^2 + L_b c_{1b}^2}{L_a+L_b} - \frac{1}{8\pi}\frac{\left(E_{-}^{0}-E_{+}^{0}\right)^2\left(F_{-}^{\alpha}+F_{-}^{\beta}\right)\left(F_{+}^{\alpha}+F_{+}^{\beta}\right)}{F_{-}^{\alpha}+F_{+}^{\alpha}+F_{-}^{\beta}+F_{+}^{\beta}} \\
&\quad + \frac{E_{-}^{0}\left(F_{-}^{\alpha}+F_{-}^{\beta}\right) + E_{+}^{0}\left(F_{+}^{\alpha}+F_{+}^{\beta}\right)}{F_{-}^{\alpha}+F_{+}^{\alpha}+F_{-}^{\beta}+F_{+}^{\beta}} n + \frac{2\pi}{F_{-}^{\alpha}+F_{+}^{\alpha}+F_{-}^{\beta}+F_{+}^{\beta}} n^2.
\end{aligned} \tag{4.90}$$

Calculation of the Background Field Configuration

To calculate the energy density, we again lack the energies E_{-}^{0} and E_{+}^{0}. By linearizing the potentials c_{1j} as proposed in eq.(4.43), we use the result found in eq.(4.47) for E_{-}^{0} and with the same linearization procedure of the energy E_{+}^{0} we obtain the correction for the upper energy. These considerations yield

$$\begin{aligned}
E_{-}^{0} &= M - \frac{\left(L_a\gamma_{1a} + L_b\gamma_{1b}\right)\Lambda}{L_a+L_b} n, \\
E_{+}^{0} &= M + \frac{\left(L_a\gamma_{1a} + L_b\gamma_{1b}\right)\Lambda}{L_a+L_b} n,
\end{aligned} \tag{4.91}$$

which gives us the energy density for four filled hole pockets up to $\mathcal{O}(n^2)$

$$\epsilon = \epsilon_0 + Mn + \left(\frac{2\rho_s(L_a\gamma_{1a}^2 + L_b\gamma_{1b}^2)}{L_a+L_b} - \frac{M_{\text{eff}}\Lambda^2(L_a\gamma_{1a}+L_b\gamma_{1b})^2}{\pi(L_a+L_b)^2} + \frac{\pi}{4M_{\text{eff}}}\right) n^2. \tag{4.92}$$

According to eq.(4.49), the variation of ϵ with respect to both potentials γ_{1j} and both lengths L_j leads to

$$\gamma_{1a} = \gamma_{1b} = 0, \tag{4.93}$$

and thus

$$c_{1a} = c_{1b} = 0. \tag{4.94}$$

Therefore, the case for two sections and four filled hole pockets also reproduces the result for a single potential c_1 leading to the homogeneous phase as previously seen in section 3.3.2.

4.2.2 Three Sections

In this subsection we follow the calculations performed in subsection 4.1.2. We also consider a periodic potential consisting of three constant sections under the condition eq.(4.52) shown in figure 4.1.2.

Magnonic Contribution to the Energy

Again, as the magnonic contribution to the energy density does not depend on the number of filled hole pockets, we have the magnonic energy density calculated in eq.(4.53)

$$\epsilon_m = 2\rho_s \frac{L_a c_{1a}^2 + L_b c_{1b}^2 + L_c c_{1c}^2}{L_a + L_b + L_c}. \tag{4.95}$$

Fermionic Contribution to the Energy

The fermionic contribution to the energy is then calculated analogously to the one in subsection 4.1.2. The minor adjustments to be made again concern the involvement of all four hole pockets and hence both energies $E_\pm^f$ for each flavor.

The hole field still needs to satisfy the conditions established in eq.(4.59). The procedure to solve that problem is again analogous to the two pocket-case and leads to the function $f_\pm^f(E_\pm^f, q, p_2)$

$$\begin{aligned}
&f_\pm^f(E_\pm^f, q, p_2) = \\
&2\cos\left(\frac{(L_a+L_b+L_c)\,(M''q + M' p_2 \sigma_f)}{M''}\right) - 2\cos\left(\frac{L_a r_{1a\pm}^f}{M''}\right)\cos\left(\frac{L_b r_{1b\pm}^f}{M''}\right)\cos\left(\frac{L_c r_{1c\pm}^f}{M''}\right) \\
&\quad + \frac{\sin\left(\frac{L_a r_{1a\pm}^f}{M''}\right)\sin\left(\frac{L_b r_{1b\pm}^f}{M''}\right)\cos\left(\frac{L_c r_{1c\pm}^f}{M''}\right)\left((r_{1a\pm}^f)^2 + (r_{1b\pm}^f)^2\right)}{r_{1a\pm}^f r_{1b\pm}^f} \\
&\quad + \frac{\sin\left(\frac{L_a r_{1a\pm}^f}{M''}\right)\cos\left(\frac{L_b r_{1b\pm}^f}{M''}\right)\sin\left(\frac{L_c r_{1c\pm}^f}{M''}\right)\left((r_{1a\pm}^f)^2 + (r_{1c\pm}^f)^2\right)}{r_{1a\pm}^f r_{1c\pm}^f} \\
&\quad + \frac{\cos\left(\frac{L_a r_{1a\pm}^f}{M''}\right)\sin\left(\frac{L_b r_{1b\pm}^f}{M''}\right)\sin\left(\frac{L_c r_{1c\pm}^f}{M''}\right)\left((r_{1b\pm}^f)^2 + (r_{1c\pm}^f)^2\right)}{r_{1b\pm}^f r_{1c\pm}^f}.
\end{aligned} \tag{4.96}$$

Again, expanding the function $f_\pm^f(E_\pm^f, q, p_2)$ around the lowest energy according to eq.(4.27) up to $\mathcal{O}(p^2)$ and proceeding as in subsection 4.2.1, we identify the total energy density up to $\mathcal{O}(n^2)$ in a straightforward manner as

$$\begin{aligned}
\epsilon \;=\; & \epsilon_0 + 2\rho_s \frac{L_a^2 c_{1a}^2 + L_b c_{1b}^2 + L_c c_{1c}^2}{L_a + L_b + L_c} - \frac{1}{8\pi}\frac{\left(E_-^0 - E_+^0\right)^2\left(F_-^\alpha + F_-^\beta\right)\left(F_+^\alpha + F_+^\beta\right)}{F_-^\alpha + F_+^\alpha + F_-^\beta + F_+^\beta} \\
& + \frac{E_-^0\left(F_-^\alpha + F_-^\beta\right) + E_+^0\left(F_+^\alpha + F_+^\beta\right)}{F_-^\alpha + F_+^\alpha + F_-^\beta + F_+^\beta} n + \frac{2\pi}{F_-^\alpha + F_+^\alpha + F_-^\beta + F_+^\beta} n^2.
\end{aligned} \tag{4.97}$$

Calculation of the Background Field Configuration

The linearization of the potentials c_{1j} according to eq.(4.43) and the identification of the energies $E^0_\pm$ according to (4.91) then gives us the energy density

$$\epsilon = \epsilon_0 + Mn + \left(\frac{2\rho_s(L_a\gamma_{1a}^2 + L_b\gamma_{1b}^2 + L_c\gamma_{1c}^2)}{L_a + L_b + L_c} - \frac{M_{\text{eff}}\Lambda^2(L_a\gamma_{1a} + L_b\gamma_{1b} + L_c\gamma_{1c})^2}{\pi(L_a + L_b + L_c)^2} + \frac{\pi}{4M_{\text{eff}}} \right) n^2. \tag{4.98}$$

The variation of the energy density according to (4.49) yields

$$\gamma_{1a} = \gamma_{1b} = \gamma_{1c} = 0, \tag{4.99}$$

and thus

$$c_{1a} = c_{1b} = c_{1c} = 0. \tag{4.100}$$

It is not a big surprise that the three-potential case with four filled hole pockets also reproduces the previously seen result for a single potential c_1 in eq.(3.33) and for two potentials c_1 and c_2 in eq.(4.94) and thus a homogeneous phase is established.

4.2.3 Extrapolation for k Sections

The above calculations for four filled hole pockets in the case of a two-section potential and a three-section potential again raises the question of a general form for the problem. In this case, we also lack a mathematical proof for the k-section case. Nonetheless, due to the same locality considerations as before, there is little doubt that in this case too each added potential c_{1j} and the according length L_j will enter into the problem in a total symmetric way. The general form for the energy density up to $\mathcal{O}(n^2)$ in the four-pocket case is hence expected to read

$$\epsilon = \epsilon_0 + Mn + \left(\frac{2\rho_s \sum_j L_j\gamma_{1j}^2}{\sum_j L_j} - \frac{M_{\text{eff}}\Lambda^2(\sum_j L_j\gamma_{1j})^2}{\pi(\sum_j L_j)^2} + \frac{\pi}{4M_{\text{eff}}} \right) n^2. \tag{4.101}$$

For an arbitrarily large number of sections the variation of the energy according to eq.(4.49) then yields

$$\gamma_{1a} = \gamma_{1b} = ... = \gamma_{1k} = 0, \tag{4.102}$$

and thus

$$c_{1a} = c_{1b} = ... = c_{1k} = 0. \tag{4.103}$$

For an arbitrarily large number of sections, in the four-pocket case the system establishes a constant zero background potential causing a homogeneous phase. Since in this case we can approximate any continuous periodic background potential with this model as well, we conclude that for small doping the zero background remains the energetically most favorable configuration and for $\frac{M_{\text{eff}}\Lambda^2}{2\pi\rho_s} < 1$, the system always establishes the homogeneous phase.

Chapter 5

Conclusion and Outlook

In this thesis, we systematically investigated the effect of a periodic potential in one lattice direction on the background field configurations for different low-energy parameters for an infinitesimally doped antiferromagnet, while setting the background potential in the other lattice direction to zero. This was a legitimate simplification because, if the system is given the opportunity to chose two arbitrary constant potentials in both directions of the lattice, it always establishes a configuration where at least one of the potentials is set to zero. We found that in the range of $1 > \frac{M_{\text{eff}}\Lambda^2}{2\pi\rho_s}$, where the energetically most favorable case is the one with four filled hole pockets, for each section of the potential the system chooses a zero potential. This causes the homogeneous phase of the staggered magnetization. In the range of $2 > \frac{M_{\text{eff}}\Lambda^2}{2\pi\rho_s} > 1$, however, only two pockets are populated with holes and for each section the system chooses a potential of $|c_j| = \frac{\Lambda}{4\rho_s}n$, thus the background potential is again constant. This case leads to a zero-degree spiral along one lattice axis in the staggered magnetization. The case of $\frac{M_{\text{eff}}\Lambda^2}{2\pi\rho_s} > 2$ has not been discussed in this thesis because the system is no longer stable in that region.

Obviously, the stripes that occur in real antiferromagnets were not obtained with these considerations. As a next task, one could try to solve the same problem for finite doping with holes. However, this problem would no longer be solvable analytically and would therefore need numerical investigations. Another future task could be the embedding of impurities in the infinitesimal doping into the theory. This would describe a real antiferromagnet more appropriately and could therefore lead to new and more exciting results. Furthermore, one could also try to include long-range Coulomb interactions into the theory as they might be the original cause of the stripes as well.

Acknowledgements

First and foremost, my thanks go to Prof. Uwe-Jens Wiese, who was an excellent supervisor during my diploma thesis. Thanks to his understanding of bigger as well as of smaller issues, he was very supportive and a great encouragement to me.
I would also like to thank the other members of the group, especially Florian Kämpfer and Christoph Brügger, who always found time to answer my questions despite their own theses. These discussions in our coffee room or over a glass of beer in a bar were very valuable to me. Moreover, I don't want to miss the opportunity to thank Otilia Hänni and Ruth Bestgen for their help in bureaucratic issues all the way through my studies here in Bern.
A big thank you also goes to the B-floor of the ExWi. I was very grateful for the harmonious working atmosphere among the diploma students. In particular, I'd like to mention Stefan Lanz, to whom I owe the solution of many minor and major problems concerning physics, computers, or the supply of wine at FKFF-meetings. In addition to this, a special note of appreciation goes to my former B70-office-mate, quantum field theory tutor, and FKFF-fellow Lorenzo Mercolli, who was sometimes the only living soul in the depths of the ExWi besides me.
I would also like to mention the non-theorists of our year, especially Andreas Gertsch. In exchange for physical knowledge, he was very inspiring in fashion matters, which should never be underestimated.
Special thanks also go to a member of the Institute for Applied Mathematics, graduate student Kaspar Riesen, for discussing my questions concerning numerical computation and for supplying me with food and entertainment every Sunday evening.
And last but not least, I am greatly obliged to Barbara Bürki, who proofread this thesis, enhancing it with a very idiomatic touch.

Appendix A

Construction of the Hamiltonian in Momentum Space

In this appendix, we work out in detail how one gets from the Hamiltonian H presented in eq.(3.9) to the matrix-valued Hamiltonian $H^f = H^f(p)$ in eq.(3.11).

$$\begin{aligned} H = \int d^2x \sum_{\substack{f=\alpha,\beta \\ s=+,-}} \Big[& M\Psi_s^{f\dagger}\Psi_s^f + \frac{1}{2M'} D_i\Psi_s^{f\dagger} D_i\Psi_s^f \\ & + \sigma_f \frac{1}{2M''}(D_1\Psi_s^{f\dagger} D_2\Psi_s^f + D_2\Psi_s^{f\dagger} D_1\Psi_s^f) \\ & + \Lambda(\Psi_s^{f\dagger} v_1^s \Psi_{-s}^f + \sigma_f \Psi_s^{f\dagger} v_2^s \Psi_{-s}^f)\Big] \end{aligned} \tag{A.1}$$

$\Psi^\dagger$ and Ψ are creation and annihilation operators. Consider the covariant derivative D_i

$$D_i\Psi_\pm^f = \partial_i\Psi_\pm^f \pm i v_i^3 \Psi_\pm^f. \tag{A.2}$$

To distinguish the operators in real space and momentum space the following convention is used

$$\begin{aligned} \Psi_\pm^{f\dagger} &= \Psi_\pm^{f\dagger}(\vec{x}) & \Psi_\pm^f &= \Psi_\pm^f(\vec{x}) \\ \widetilde{\Psi}_\pm^{f\dagger} &= \widetilde{\Psi}_\pm^{f\dagger}(\vec{p}) & \widetilde{\Psi}_\pm^f &= \widetilde{\Psi}_\pm^f(\vec{p}). \end{aligned} \tag{A.3}$$

Write

$$\begin{aligned} \Psi_s^{f\dagger} &= \frac{1}{(2\pi)^2}\int d^2p\; e^{i\vec{p}\cdot\vec{x}}\widetilde{\Psi}_s^{f\dagger} \\ \Psi_s^f &= \frac{1}{(2\pi)^2}\int d^2p\; e^{-i\vec{p}\cdot\vec{x}}\widetilde{\Psi}_s^f. \end{aligned} \tag{A.4}$$

The covariant derivative acts on the operators as

$$\begin{aligned} D_i\Psi_\pm^f &= \partial_i\Psi_\pm^f \pm i v_i^3\Psi_\pm^f \\ &= \partial_i \frac{1}{(2\pi)^2}\int d^2p\; e^{-i\vec{p}\cdot\vec{x}}\widetilde{\Psi}_\pm^f \pm i v_i^3 \frac{1}{(2\pi)^2}\int d^2p\; e^{-i\vec{p}\cdot\vec{x}}\widetilde{\Psi}_\pm^f \\ &= \frac{1}{(2\pi)^2}\int d^2p\; (-ip_i)e^{-i\vec{p}\cdot\vec{x}}\widetilde{\Psi}_\pm^f \pm i v_i^3 \frac{1}{(2\pi)^2}\int d^2p\; e^{-i\vec{p}\cdot\vec{x}}\widetilde{\Psi}_\pm^f \\ &= \frac{1}{(2\pi)^2}\int d^2p\; (-ip_i \pm i v_i^3)e^{-i\vec{p}\cdot\vec{x}}\widetilde{\Psi}_\pm^f. \end{aligned} \tag{A.5}$$

The kinetic term in the Lagrangian reads

$$\begin{aligned} D_i\Psi_\pm^{f\dagger} D_i\Psi_\pm^f &= \left[(\partial_i \pm iv_i^3)\Psi_\pm^f\right]^\dagger (\partial_i \pm iv_i^3)\Psi_\pm^f \\ &= (\partial_i\Psi_\pm^{f\dagger} \mp iv_i^3\Psi_\pm^{f\dagger})(\partial_i\Psi_\pm^f \pm iv_i^3\Psi_\pm^f) \\ &= \partial_i\Psi_\pm^{f\dagger}\partial_i\Psi_\pm^{f\dagger} \pm iv_i^3(\partial_i\Psi_\pm^{f\dagger})\Psi_\pm^f \mp iv_i^3\Psi_\pm^{f\dagger}(\partial_i\Psi_\pm^f) - (iv_i^3)^2\Psi_\pm^{f\dagger}\Psi_\pm^f. \end{aligned} \tag{A.6}$$

Using partial integration the following terms in the Hamiltonian arise

$$\begin{aligned} \int d^2x\ (\partial_i\Psi_\pm^{f\dagger})(\partial_i\Psi_\pm^f) &= \underbrace{\Psi_\pm^{f\dagger}(\partial_i\Psi_\pm^f)\Big|_{-\infty}^{\infty}}_{=0} - \int d^2x\ \Psi_\pm^{f\dagger}(\partial_i^2\Psi_\pm^f) \\ &= -\int d^2x\ \Psi_\pm^{f\dagger}(\partial_i^2\Psi_\pm^f) \\ \int d^2x\ (\partial_i\Psi_\pm^{f\dagger})\Psi_\pm^f &= \underbrace{\Psi_\pm^{f\dagger}\Psi_\pm^f\Big|_{-\infty}^{\infty}}_{=0} - \int d^2x\ \Psi_\pm^{f\dagger}(\partial_i\Psi_\pm^f) \\ &= -\int d^2x\ \Psi_\pm^{f\dagger}(\partial_i\Psi_\pm^f). \end{aligned} \tag{A.7}$$

It is then possible to rewrite eq.(A.6) as follows

$$\begin{aligned} D_i\Psi_\pm^{f\dagger} D_i\Psi_\pm^f &= \partial_i\Psi_\pm^{f\dagger}\partial_i\Psi_\pm^{f\dagger} \pm iv_i^3(\partial_i\Psi_\pm^{f\dagger})\Psi_\pm^f \mp iv_i^3\Psi_\pm^{f\dagger}(\partial_i\Psi_\pm^f) + (v_i^3)^2\Psi_\pm^{f\dagger}\Psi_\pm^f \\ &= -\Psi_\pm^{f\dagger}(\partial_i^2\Psi_\pm^f) \mp iv_i^3\Psi_\pm^{f\dagger}(\partial_i\Psi_\pm^f) \mp iv_i^3\Psi_\pm^{f\dagger}(\partial_i\Psi_\pm^f) - (iv_i^3)^2\Psi_\pm^{f\dagger}\Psi_\pm^f \\ &= -\Psi_\pm^{f\dagger}(\partial_i \pm iv_i^3)^2\Psi_\pm^f \\ &= -\Psi_\pm^{f\dagger} D_i D_i\Psi_\pm^f. \end{aligned} \tag{A.8}$$

The Hamiltonian can therefore be written as

$$\begin{aligned} H = \int d^2x \sum_{\substack{f=\alpha,\beta \\ s=+,-}} \Big[& M\Psi_s^{f\dagger}\Psi_s^f - \frac{1}{2M'}\Psi_s^{f\dagger} D_i D_i\Psi_s^f \\ & - \sigma_f\frac{1}{2M''}\left(\Psi_s^{f\dagger} D_1 D_2\Psi_s^f + \Psi_s^{f\dagger} D_2 D_1\Psi_s^f\right) \\ & + \Lambda(\Psi_s^{f\dagger} v_1^s\Psi_{-s}^f + \sigma_f\Psi_s^{f\dagger} v_2^s\Psi_{-s}^f)\Big]. \end{aligned} \tag{A.9}$$

If four-fermi couplings are neglected, the flavors α and β are independent. Hence, it is allowed to separate the Hamiltonian into two contributions

$$\begin{aligned} H^f = \int d^2x \sum_{s=+,-} \Big[& M\Psi_s^{f\dagger}\Psi_s^f - \frac{1}{2M'}\Psi_s^{f\dagger} D_i D_i\Psi_s^f \\ & - \sigma_f\frac{1}{2M''}\left(\Psi_s^{f\dagger} D_1 D_2\Psi_s^f + \Psi_s^{f\dagger} D_2 D_1\Psi_s^f\right) \\ & + \Lambda\left(\Psi_s^{f\dagger} v_1^s\Psi_{-s}^f + \sigma_f\Psi_s^{f\dagger} v_2^s\Psi_{-s}^f\right)\Big]. \end{aligned} \tag{A.10}$$

Plugging the relation eq.(A.4) in the above eq.(A.10) we get

$$\begin{aligned} H^f = \frac{1}{(2\pi)^4}\int d^2x \int d^2p'\ d^2p \sum_{s=+,-} \Big[& M e^{i\vec{p'}\cdot\vec{x}} \widetilde{\Psi}_s^{f\dagger}(\vec{p'})\ e^{-i\vec{p}\cdot\vec{x}} \widetilde{\Psi}_s^f(\vec{p}) \\ & - \frac{1}{2M'} e^{i\vec{p'}\cdot\vec{x}} \widetilde{\Psi}_s^{f\dagger}(\vec{p'})(-ip_i \pm isv_i^3)^2\ e^{-i\vec{p}\cdot\vec{x}} \widetilde{\Psi}_s^f(\vec{p}) \\ & - \sigma_f \frac{1}{2M'} \Big(e^{i\vec{p'}\cdot\vec{x}} \widetilde{\Psi}_s^{f\dagger}(\vec{p'})(-ip_1 \pm isv_1^3)(-ip_2 \pm isv_2^3)\ e^{-i\vec{p}\cdot\vec{x}} \widetilde{\Psi}_s^f(\vec{p}) \\ & \qquad + e^{i\vec{p'}\cdot\vec{x}} \widetilde{\Psi}_s^{f\dagger}(\vec{p'})(-ip_2 \pm isv_2^3)(-ip_1 \pm isv_1^3)\ e^{-i\vec{p}\cdot\vec{x}} \widetilde{\Psi}_s^f(\vec{p}) \Big) \\ & + \Lambda \Big(e^{i\vec{p'}\cdot\vec{x}} \widetilde{\Psi}_s^{f\dagger}(\vec{p'}) v_1^s\ e^{-i\vec{p}\cdot\vec{x}} \widetilde{\Psi}_{-s}^f(\vec{p}) + \sigma_f e^{i\vec{p'}\cdot\vec{x}} \widetilde{\Psi}_s^{f\dagger}(\vec{p'}) v_2^s\ e^{-i\vec{p}\cdot\vec{x}} \widetilde{\Psi}_{-s}^f(\vec{p}) \Big) \Big]. \end{aligned} \tag{A.11}$$

Since we have

$$\begin{aligned} \int d^2x \int d^2p' \int d^2p\ e^{-i(\vec{p'}-\vec{p})\vec{x}} &= \int d^2p' \int d^2p\ \delta(\vec{p'}-\vec{p})(2\pi)^2 \\ &= \int d^2p\ (2\pi)^2, \end{aligned} \tag{A.12}$$

we can rewrite eq.(A.11) as follows

$$\begin{aligned} H^f = \frac{1}{(2\pi)^2}\int d^2p \sum_{s=+,-} \Big[& M \widetilde{\Psi}_s^{f\dagger} \widetilde{\Psi}_s^f - \frac{1}{2M'} \widetilde{\Psi}_s^{f\dagger}(-ip_i \pm isv_i^3)^2 \widetilde{\Psi}_s^f \\ & - \sigma_f \frac{1}{2M''} \Big(\widetilde{\Psi}_s^{f\dagger}(-ip_1 \pm isv_1^3)(-ip_2 \pm isv_2^3) \widetilde{\Psi}_s^f \\ & \qquad + \widetilde{\Psi}_s^{f\dagger}(-ip_2 \pm isv_2^3)(-ip_1 \pm isv_1^3) \widetilde{\Psi}_s^f \Big) \\ & + \Lambda \Big(\widetilde{\Psi}_s^{f\dagger} v_1^s \widetilde{\Psi}_{-s}^f + \sigma_f \widetilde{\Psi}_s^{f\dagger} v_2^s \widetilde{\Psi}_{-s}^f \Big) \Big]. \end{aligned} \tag{A.13}$$

Consider now the factors due to the derivative in real space

$$\begin{aligned} (-ip_i \pm isv_i^3)^2 &= -(p_i \mp sv_i^3)^2, \\ (-ip_1 \pm isv_1^3)(-ip_2 \pm isv_2^3) &= -(p_1 \mp sv_1^3)(p_2 \mp sv_2^3), \\ (-ip_2 \pm isv_2^3)(-ip_1 \pm isv_1^3) &= -(p_2 \mp sv_2^3)(p_1 \mp sv_1^3). \end{aligned} \tag{A.14}$$

Using the gauge transformation suggested in eq.(3.1), we replace

$$v_i^3(\vec{x})' = c_i^3, \qquad \text{and} \qquad v_i^{\pm}(\vec{x}) = c_i. \tag{A.15}$$

In this case, the factors $(p_i \mp sv_i^3)(p_j \mp sv_j^3),\ i,j,\in\{1,2\}$ commute, which makes it possible to rewrite the Hamiltonian as

$$\begin{aligned}
H^f = \frac{1}{(2\pi)^2}\int d^2p \sum_{s=+,-} \Big[& M\widetilde{\Psi}_s^{f\dagger}\widetilde{\Psi}_s^f + \frac{1}{2M'}\widetilde{\Psi}_s^{f\dagger}(p_i \mp sc_i^3)^2\widetilde{\Psi}_s^f) \\
& + \sigma_f \frac{1}{2M''}\Big(\widetilde{\Psi}_s^{f\dagger}(p_1 \mp sc_1^3)(p_2 \mp sc_2^3)\widetilde{\Psi}_s^f \\
& \qquad + \widetilde{\Psi}_s^{f\dagger}(p_2 \mp sc_2^3)(p_1 \mp sc_1^3)\widetilde{\Psi}_s^f\Big) \\
& + \Lambda\left(\widetilde{\Psi}_s^{f\dagger}c_1\widetilde{\Psi}_{-s}^f + \sigma_f\widetilde{\Psi}_s^{f\dagger}c_2\widetilde{\Psi}_{-s}^f\right)\Big] \\
= \frac{1}{(2\pi)^2}\int d^2p \sum_{s=+,-} \Big[& M\widetilde{\Psi}_s^{f\dagger}\widetilde{\Psi}_s^f - \frac{(p_i \mp sc_i^3)^2}{2M'}\widetilde{\Psi}_s^{f\dagger}\widetilde{\Psi}_s^f \\
& + \sigma_f\frac{(p_2 \mp sc_2^3)(p_1 \mp sc_1^3)}{M''}\widetilde{\Psi}_s^{f\dagger}\widetilde{\Psi}_s^f \\
& + \Lambda(c_1 + \sigma_f c_2)\widetilde{\Psi}_s^{f\dagger}\widetilde{\Psi}_{-s}^f\Big].
\end{aligned} \tag{A.16}$$

Consider now the sum of the integrand

$$\begin{aligned}
& \sum_{s=+,-}\Big[M\widetilde{\Psi}_s^{f\dagger}\widetilde{\Psi}_s^f + \frac{(p_i \mp sc_i^3)^2}{2M'}\widetilde{\Psi}_s^{f\dagger}\widetilde{\Psi}_s^f + \sigma_f\frac{(p_2 \mp sc_2^3)(p_1 \mp sc_1^3)}{M''}\widetilde{\Psi}_s^{f\dagger}\widetilde{\Psi}_s^f \\
& \qquad + \Lambda(c_1 + \sigma_f c_2)\widetilde{\Psi}_s^{f\dagger}\widetilde{\Psi}_{-s}^f\Big] \\
& = \widetilde{\Psi}_+^{f\dagger}\left(M + \frac{(p_i - c_i^3)^2)}{2M''} + \sigma_f\frac{(p_1 - c_1^3)(p_2 - c_2^3)}{M''}\right)\widetilde{\Psi}_+^f + \widetilde{\Psi}_+^{f\dagger}\Lambda(c_1 + \sigma_f c_2)\widetilde{\Psi}_-^f \\
& \quad + \widetilde{\Psi}_-^{f\dagger}\left(M + \frac{(p_i + c_i^3)^2}{2M''} + \sigma_f\frac{(p_1 + c_1^3)(p_2 + c_2^3)}{M''}\right)\widetilde{\Psi}_-^f + \widetilde{\Psi}_-^{f\dagger}\Lambda(c_1 + \sigma_f c_2)\widetilde{\Psi}_+^f \\
& = \widetilde{\Psi}_+^{f\dagger}A\widetilde{\Psi}_+^f + \widetilde{\Psi}_+^{f\dagger}B\widetilde{\Psi}_-^f + \widetilde{\Psi}_-^{f\dagger}C\widetilde{\Psi}_-^f + \widetilde{\Psi}_-^{f\dagger}D\widetilde{\Psi}_+^f,
\end{aligned} \tag{A.17}$$

using the abbreviation

$$\begin{aligned}
A &= M + \frac{(p_i - c_i^3)^2}{2M''} + \sigma_f\frac{(p_1 - c_1^3)(p_2 - c_2^3)}{M''}, \\
B &= \Lambda(c_1 + \sigma_f c_2), \\
C &= M + \frac{(p_i + c_i^3)^2}{2M''} + \sigma_f\frac{(p_1 + c_1^3)(p_2 + c_2^3)}{M''}, \\
D &= \Lambda(c_1 + \sigma_f c_2).
\end{aligned} \tag{A.18}$$

The latter form can be written as a matrix multiplication

$$\left(\widetilde{\Psi}_+^{f\dagger}, \widetilde{\Psi}_-^{f\dagger}\right)\begin{pmatrix} A & B \\ C & D \end{pmatrix}\begin{pmatrix} \widetilde{\Psi}_+^f \\ \widetilde{\Psi}_-^f \end{pmatrix}. \tag{A.19}$$

In shorthand notation, we therefore write

$$H^f = \langle\widetilde{\Psi}^f|H^f(p)|\widetilde{\Psi}^f\rangle, \tag{A.20}$$

denoting the Hamiltonian

$$H^f(p) = \begin{pmatrix} M + \frac{(p_i - c_i^3)^2}{2M'} + \sigma_f \frac{(p_1 - c_1^3)(p_2 - c_2^3)}{M''} & \Lambda(c_1 + \sigma_f c_2) \\ \Lambda(c_1 + \sigma_f c_2) & M + \frac{(p_i + c_i^3)^2}{2M'} + \sigma_f \frac{(p_1 + c_1^3)(p_2 + c_2^3)}{M''} \end{pmatrix}, \quad \text{(A.21)}$$

which is equal to the Hamiltonian in eq.(3.11).

Appendix B

Construction of the Reciprocal Lattice

B.1 1-Dimensional Case

Assume a 1-dimensional periodic lattice with N sites and with periodic boundary conditions such that the site N equals the site 0. Define

$$\delta_{nn'} = \frac{1}{N} \sum_{j=0}^{N-1} e^{2\pi i \frac{n-n'}{N} j}. \tag{B.1}$$

The $\delta_{nn'}$ then has the standard Kronecker property

$$\frac{1}{N} \sum_{j=0}^{N-1} e^{2\pi i \frac{n-n'}{N} j} = \begin{cases} 1 & n = n' \\ 0 & n \neq n' \end{cases} \tag{B.2}$$

and also represents the periodicity of the lattice. For $n \Rightarrow n + mN,\ m \in \mathbb{Z}$, we have

$$\begin{aligned} \frac{1}{N} \sum_{j=0}^{N-1} e^{2\pi i \frac{n+mN-(n'+m'N)}{N} j} &= \frac{1}{N} \sum_{j=0}^{N-1} e^{2\pi i \frac{n-n'}{N} j} e^{2\pi i \frac{m-m'}{N} Nj} \\ &= \frac{1}{N} \sum_{j=0}^{N-1} e^{2\pi i \frac{n-n'}{N} j}. \end{aligned} \tag{B.3}$$

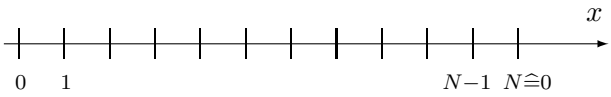

Figure B.1: A 1-dimensional periodic lattice with lattice spacing a and N sites.

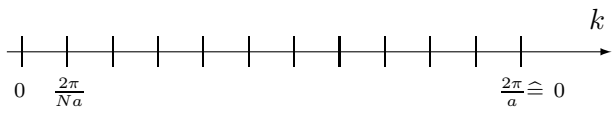

Figure B.2: The momentum lattice for a periodic real space lattice with lattice spacing a and N sites.

Therefore, we can write

$$\begin{aligned}
\psi_n &= \sum_{n'} \delta_{nn'} \psi_{n'} \\
&= \sum_{n'=0}^{N-1} \frac{1}{N} \sum_{j=0}^{N-1} e^{2\pi i \frac{n-n'}{N} j} \psi_{n'} \\
&= \sum_{j=0}^{N-1} e^{2\pi i \frac{n}{N} j} \frac{1}{N} \sum_{n'=0}^{N-1} e^{-2\pi i \frac{n'}{N} j} \psi_{n'} \\
&= \sum_{j=0}^{N-1} e^{2\pi i \frac{n}{N} j} \widetilde{\psi}_j, \qquad \widetilde{\psi}_j = \frac{1}{N} \sum_{n'=0}^{N-1} e^{-2\pi i \frac{n'}{N} j} \psi_{n'}.
\end{aligned} \tag{B.4}$$

Since the lattice is discrete with spacing a between the sites, we can replace the sites n by $x = na$:

$$\psi_x = \sum_{j=0}^{N-1} e^{2\pi i \frac{x}{Na} j} \widetilde{\psi}_j. \tag{B.5}$$

Renaming

$$k_j = \frac{2\pi}{Na} j, \tag{B.6}$$

we can rewrite the above equation as follows

$$\psi_x = \sum_{j=0}^{N-1} e^{i k_j x} \widetilde{\psi}_{k_j} \tag{B.7}$$

or simply as a summation over the momenta

$$\psi_x = \sum_{k} e^{ikx} \widetilde{\psi}_k, \tag{B.8}$$

which is the commonly used representation of a discrete Fourier transformation. From eq.(B.6), it follows further that a periodic lattice with spacing a and N sites generates a reciprocal lattice in momentum space with a discrete set of N momenta k_j in the interval $[0, \frac{2\pi}{a}]$. We call k a reciprocal lattice vector. Note also that due to the periodicity of the lattice

$$e^{ik(mNa)} = 1, \qquad m \in \mathbb{Z}. \tag{B.9}$$

B.2 2-Dimensional Case

The 2-dimensional case works analogously to the 1-dimensional case. For the discrete Fourier transformation we write

$$\psi_{\vec{x}} = \sum_{\vec{k}} e^{i\vec{k}\cdot\vec{x}} \widetilde{\psi}_{\vec{k}}. \tag{B.10}$$

Denoting any linear combination of the basis vectors $\vec{a}_i$ in the direct lattice by $\vec{G}$,

$$\vec{G} = m_1\vec{a}_1 + m_2\vec{a}_2, \qquad m_i \in \mathbb{Z}, \tag{B.11}$$

the equivalent relation to eq.(B.9) must hold

$$e^{i\vec{k}\cdot\vec{G}} = 1. \tag{B.12}$$

Let us define the reciprocal vectors $\vec{k}$ through the basis vectors of the reciprocal lattice $\vec{g}_i,\ i \in \{1,2\}$,

$$\vec{k} = l_1\vec{g}_1 + l_2\vec{g}_2, \qquad l_i \in \mathbb{Z}. \tag{B.13}$$

It then follows, due to eq.(B.12), that the basis vectors of the direct lattice $\vec{a}_i$ and the basis vectors of the reciprocal lattice $\vec{g}_i$ must satisfy the following set of equations

$$\vec{a}_i \cdot \vec{g}_j = 2\pi\delta_{ij}. \tag{B.14}$$

B.3 The 2-Dimensional Lattice of the Theory

We apply this concept to the sublattices of this theory. According to figure B.3, the basis vectors of the sublattice $X \in \{A, B, ..., H\}$ can be chosen as follows

$$\vec{a}_1 = \begin{pmatrix} 4a \\ 0 \end{pmatrix}, \qquad \text{and} \qquad \vec{a}_2 = \begin{pmatrix} 2a \\ 2a \end{pmatrix}. \tag{B.15}$$

Satisfying eq.(B.14), the following basis of the reciprocal lattice $\vec{g}_i$ can be constructed

$$\vec{g}_1 = \begin{pmatrix} 0 \\ \frac{\pi}{a} \end{pmatrix}, \qquad \text{and} \qquad \vec{g}_2 = \begin{pmatrix} \frac{\pi}{2a} \\ -\frac{\pi}{2a} \end{pmatrix}. \tag{B.16}$$

The resulting reciprocal lattice is shown in figure (B.4), providing momenta at $k = (\pm\frac{\pi}{2a}, \pm\frac{\pi}{2a})$, where they indeed occur in cuprates.

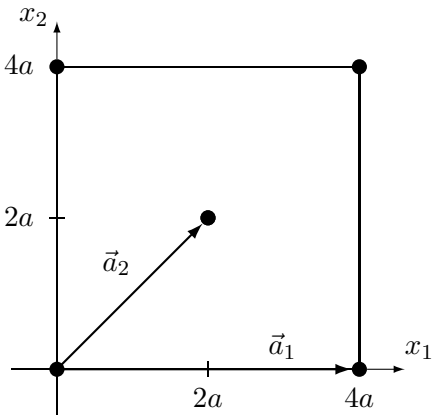

Figure B.3: The sublattice for each field configuration $\psi^X(x),\ X \in \{A, B, ..., H\}$, with the according basis vectors $\vec{a}_i$, $i \in \{1, 2\}$, in real space. The lattice spacing of the complete lattice consisting of all the different sublattices X, is a. For the complete lattice see also figure (2.1).

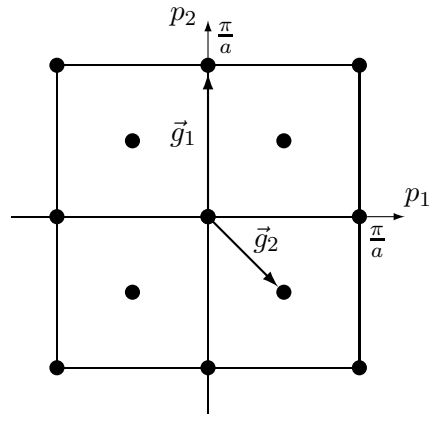

Figure B.4: The reciprocal lattice for lattice X in real space with the according momenta and their periodic copies and the basis vectors $\vec{g}_i$, $i \in \{1, 2\}$.

Appendix C

$[D, H] = 0$ for a Periodic Potential $V(x)$

In the derivation of the two-potential problem in chapter 4, the fact that the Hamiltonian H with a periodic potential and the displacement operator D have the same eigenvectors has been used. The statement that H and D do have the same eigenvectors is equivalent to the statement that both operators commute. This is exactly what is shown in this appendix.

The potential $V(x)$ is periodic, hence

$$V(x) = V(x + l). \tag{C.1}$$

The displacement operator D acts on a wave function as follows

$$^{D}\psi(x) = \psi(x + l). \tag{C.2}$$

Therefore, the operators H and D commute

$$\begin{aligned}
[D, H(x)]\psi(x) &= {}^{D}\left(H(x)\psi(x)\right) - H(x)^{D}\psi(x) \\
&= {}^{D}\left(-\frac{1}{2m}\psi''(x) + V(x)\psi(x)\right) - H(x)\psi(x + l) \\
&= -\frac{1}{2m}\psi''(x + l) + V(x + l)\psi(x + l) \\
&\quad -\left(-\frac{1}{2m}\psi''(x + l) + V(x)\psi(x + l)\right) \\
&= 0
\end{aligned} \tag{C.3}$$

Hence, it is justified to choose the eigenvectors for H and for D to be the same ones.

Appendix D

Derivatives of $f^f_\pm(E^f_\pm, q, p_2)$

Considering eq.(4.6), which implies that $E^\alpha_\pm(0,0) = E^\beta_\pm(0,0) = E^0_\pm$, and defining

$$R_{1j\pm} = \sqrt{2M'(E^0_\pm - M \mp \Lambda c_{1j})}, \quad j \in \{a, b, c\}, \tag{D.1}$$

we write down the derivatives of the function $f^f_\pm(E^f_\pm, q, p_2)$.

D.1 Two Sections

$$\begin{aligned}
\frac{\partial^2}{\partial p_2^2} f^f_\pm(E^0_\pm, 0, 0) &= (L_a + L_b)^2 \frac{M'^2}{M''^2} \\
&+ \frac{M'^2}{2M^2_{\text{eff}}} \Bigg\{ \frac{L_a \cos(L_b R_{1b\pm}) \sin(L_a R_{1a\pm})}{R_{1a\pm}} \\
&+ \frac{L_b \cos(L_a R_{1a\pm}) \sin(L_b R_{1b\pm})}{R_{1b\pm}} \\
&+ \frac{2 \sin(L_a R_{1a\pm}) \sin(L_b R_{1b\pm})}{R_{1a\pm} R_{1b\pm}} \\
&+ \frac{L_b \sin(L_a R_{1b\pm}) \sin(L_a R_{1a\pm}) (R^2_{1a\pm} + R^2_{1b\pm})}{R_{1a\pm} R^2_{1b\pm}} \\
&+ \frac{L_a \cos(L_a R_{1a\pm}) \sin(L_b R_{1b\pm}) (R^2_{1a\pm} + R^2_{1b\pm})}{R_{1b\pm} R^2_{1a\pm}} \\
&+ \frac{M' \sin(L_a R_{1a\pm}) \sin(L_b R_{1b\pm}) (R^2_{1a\pm} + R^2_{1b\pm})}{R_{1a\pm} R^3_{1b\pm}} \\
&+ \frac{M' \sin(L_a R_{1a\pm}) \sin(L_b R_{1b\pm}) (R^2_{1a\pm} + R^2_{1b\pm})}{R_{1b\pm} R^3_{1a\pm}} \Bigg\},
\end{aligned}$$

$$\frac{\partial^2}{\partial q \, \partial p_2} f^f_\pm(E^0_\pm, 0, 0) = \frac{(L_a + L_b)^2 M' \sigma_f}{M''},$$

$$
\begin{aligned}
\frac{\partial^2}{\partial q^2} f_{\pm}^{f}(E_{\pm}^{0},0,0) &= (L_a + L_b)^2\,, \\
\frac{\partial}{\partial E_{\pm}^{f}} f_{\pm}^{f}(E_{\pm}^{0},0,0) &= M'\Big\{ - \frac{L_a \cos\left(L_b R_{1b\pm}\right) \sin\left(L_a R_{1a\pm}\right)}{R_{1a\pm}} \\
&\quad - \frac{L_b \cos\left(L_a R_{1a\pm}\right) \sin\left(L_b R_{1b\pm}\right)}{R_{1b\pm}} \\
&\quad - \frac{\sin\left(L_a R_{1a\pm}\right) \sin\left(L_b R_{1b\pm}\right)}{R_{1a\pm} R_{1b\pm}} \\
&\quad - \frac{L_b \cos\left(L_b R_{1b\pm}\right) \sin\left(L_a R_{1a\pm}\right) \left(R_{1a\pm}^2 + R_{1b\pm}^2\right)}{R_{1a\pm} R_{1b\pm}^2} \\
&\quad + \frac{L_a \cos\left(L_a R_{1a\pm}\right) \sin\left(L_b R_{1b\pm}\right) \left(R_{1a\pm}^2 + R_{1b\pm}^2\right)}{R_{1b\pm} R_{1a\pm}^2} \\
&\quad - \frac{M' \sin\left(L_a R_{1a\pm}\right) \sin\left(L_b R_{1b\pm}\right) \left(R_{1a\pm}^2 + R_{1b\pm}^2\right)}{R_{1b\pm} R_{1a\pm}^3} \\
&\quad + \frac{M' \sin\left(L_a R_{1a\pm}\right) \sin\left(L_b R_{1b\pm}\right) \left(R_{1a\pm}^2 + R_{1b\pm}^2\right)}{R_{1b\pm} R_{1a\pm}^3} \Big\}. \qquad \text{(D.2)}
\end{aligned}
$$

D.2 Three Sections

$$
\begin{aligned}
\frac{\partial^2}{\partial p_2^2} f_{\pm}^{f}(E_{\pm}^{0},0,0) &= -\frac{2(L_a + L_b + L_c)^2 M'^2}{M''^2} \\
&\quad - \frac{M'^2}{M_{\text{eff}}^2} \Big\{ \frac{2L_a \cos(L_b R_{1b\pm}) \cos(L_c R_{1c\pm}) \sin(L_a R_{1a\pm})}{R_{1a\pm}} \\
&\qquad + \frac{2L_b \cos(L_a R_{1a\pm}) \cos(L_c R_{1c\pm}) \sin(L_b R_{1b\pm})}{R_{1b\pm}} \\
&\qquad + \frac{2L_c \cos(L_a R_{1a\pm}) \cos(L_b R_{1b\pm}) \sin(L_c R_{1c\pm})}{R_{1c\pm}} \\
&\qquad + \frac{4 \cos(L_c R_{1c\pm}) \sin(L_a R_{1a\pm}) \sin(L_b R_{1b\pm})}{R_{1a\pm} R_{1b\pm}} \\
&\qquad + \frac{4 \cos(L_b R_{1b\pm}) \sin(L_a R_{1a\pm}) \sin(L_c R_{1c\pm})}{R_{1a\pm} R_{1c\pm}} \\
&\qquad + \frac{4 \cos(L_a R_{1a\pm}) \sin(L_b R_{1b\pm}) \sin(L_c R_{1c\pm})}{R_{1b\pm} R_{1c\pm}} \\
&\qquad + \frac{L_a M' (R_{1a\pm}^2 + R_{1b\pm}^2) \cos(L_a R_{1a\pm}) \cos(L_c R_{1c\pm}) \sin(L_b R_{1b\pm})}{R_{1a\pm}^2 R_{1b\pm}} \\
&\qquad + \frac{L_a M' (R_{1a\pm}^2 + R_{1c\pm}^2) \cos(L_a R_{1a\pm}) \cos(L_b R_{1b\pm}) \sin(L_c R_{1c\pm})}{R_{1a\pm}^2 R_{1c\pm}} \\
&\qquad + \frac{L_b M' (R_{1a\pm}^2 + R_{1b\pm}^2) \cos(L_b R_{1b\pm}) \cos(L_c R_{1c\pm}) \sin(L_a R_{1a\pm})}{R_{1b\pm}^2 R_{1a\pm}}
\end{aligned}
$$

$$
\begin{aligned}
&+\frac{L_bM'(R_{1b\pm}^2+R_{1c\pm}^2)\cos(L_aR_{1a\pm})\cos(L_bR_{1b\pm})\sin(L_cR_{1c\pm})}{R_{1b\pm}^2R_{1c\pm}}\\
&+\frac{L_cM'(R_{1a\pm}^2+R_{1c\pm}^2)\cos(L_bR_{1b\pm})\cos(L_cR_{1c\pm})\sin(L_aR_{1a\pm})}{R_{1c\pm}^2R_{1a\pm}}\\
&+\frac{L_cM'(R_{1b\pm}^2+R_{1c\pm}^2)\cos(L_aR_{1a\pm})\cos(L_cR_{1c\pm})\sin(L_bR_{1b\pm})}{R_{1c\pm}^2R_{1b\pm}}\\
&-\frac{M'M''^2(R_{1a\pm}^2+R_{1b\pm}^2)\cos(L_cR_{1c\pm})\sin(L_aR_{1a\pm}^2)\sin(L_bR_{1b\pm}^2)}{R_{1a\pm}^3R_{1b\pm}}\\
&-\frac{M'M''^2(R_{1a\pm}^2+R_{1c\pm}^2)\cos(L_bR_{1b\pm})\sin(L_aR_{1a\pm})\sin(L_cR_{1c\pm})}{R_{1a\pm}^3R_{1c\pm}}\\
&-\frac{M'M''^2(R_{1a\pm}^2+R_{1b\pm}^2)\cos(L_cR_{1c\pm})\sin(L_aR_{1a\pm})\sin(L_bR_{1b\pm})}{R_{1b\pm}^3R_{1a\pm}}\\
&-\frac{M'M''^2(R_{1b\pm}^2+R_{1c\pm}^2)\cos(L_aR_{1a\pm})\sin(L_bR_{1b\pm})\sin(L_cR_{1c\pm})}{R_{1b\pm}^3R_{1c\pm}}\\
&-\frac{M'M''^2(R_{1a\pm}^2+R_{1c\pm}^2)\cos(L_bR_{1b\pm})\sin(L_aR_{1a\pm})\sin(L_cR_{1c\pm})}{R_{1c\pm}^3R_{1a\pm}}\\
&-\frac{M'M''^2(R_{1b\pm}^2+R_{1c\pm}^2)\cos(L_aR_{1a\pm})\sin(L_bR_{1b\pm})\sin(L_cR_{1c\pm})}{R_{1c\pm}^3R_{1b\pm}}\\
&-\frac{L_aM'(R_{1b\pm}^2+R_{1c\pm}^2)\sin(L_aR_{1a\pm})\sin(L_b1b\pm)\sin(L_cR_{1c\pm})}{R_{1a\pm}R_{1b\pm}R_{1c\pm}}\\
&-\frac{L_bM'(R_{1a\pm}^2+R_{1c\pm}^2)\sin(L_aR_{1a\pm})\sin(L_b1b\pm)\sin(L_cR_{1c\pm})}{R_{1a\pm}R_{1b\pm}R_{1c\pm}}\\
&-\frac{L_cM'(R_{1a\pm}^2+R_{1b\pm}^2)\sin(L_aR_{1a\pm})\sin(L_b1b\pm)\sin(L_cR_{1c\pm})}{R_{1a\pm}R_{1b\pm}R_{1c\pm}}\Big\},
\end{aligned}
$$

$$
\begin{aligned}
\frac{\partial^2}{\partial q\,\partial p_2}f_\pm^f(E_\pm^0,0,0) &= -\frac{2(L_a+L_b+L_c)^2M'\sigma_f}{M''},\\
\frac{\partial^2}{\partial q^2}f_\pm^f(E_\pm^0,0,0) &= -2(L_a+L_b+L_c)^2,\\
\frac{\partial}{\partial E_\pm^f}f_{E_\pm}^f(E_\pm^0,0,0) &= \frac{2L_aM'\cos(L_bR_{1b\pm})\cos(L_cR_{1c\pm})\sin(L_aR_{1a\pm})}{R_{1a\pm}}\\
&+\frac{2L_bM'\cos(L_aR_{1a\pm})\cos(L_cR_{1c\pm})\sin(L_bR_{1b\pm})}{R_{1b\pm}}\\
&+\frac{2L_cM'\cos(L_aR_{1a\pm})\cos(L_bR_{1b\pm})\sin(L_cR_{1c\pm})}{R_{1c\pm}}\\
&+\frac{4M'\cos(L_cR_{1c\pm})\sin(L_aR_{1a\pm})\sin(L_bR_{1b\pm})}{R_{1a\pm}R_{1b\pm}}\\
&+\frac{4M'\cos(L_bR_{1b\pm})\sin(L_aR_{1a\pm})\sin(L_cR_{1c\pm})}{R_{1a\pm}R_{1c\pm}}
\end{aligned}
$$

$$
\begin{aligned}
&+\frac{4M'\cos(L_aR_{1c\pm})\sin(L_bR_{1b\pm})\sin(L_cR_{1c\pm})}{R_{1b\pm}R_{1b\pm}}\\
&+\frac{L_aM'^2(R^2_{1a\pm}+R^2_{1b\pm})\cos(L_aR_{1a\pm})\cos(L_cR_{1c\pm})\sin(L_bR_{1b\pm})}{R^2_{1a\pm}R_{1b\pm}}\\
&+\frac{L_aM'^2(R^2_{1a\pm}+R^2_{1c\pm})\cos(L_aR_{1a\pm})\cos(L_bR_{1b\pm})\sin(L_cR_{1c\pm})}{R^2_{1a\pm}R_{1c\pm}}\\
&+\frac{L_bM'^2(R^2_{1a\pm}+R^2_{1b\pm})\cos(L_bR_{1b\pm})\cos(L_cR_{1c\pm})\sin(L_aR_{1a\pm})}{R^2_{1b\pm}R_{1a\pm}}\\
&+\frac{L_bM'^2(R^2_{1b\pm}+R^2_{1c\pm})\cos(L_aR_{1a\pm})\cos(L_bR_{1b\pm})\sin(L_cR_{1c\pm})}{R^2_{1b\pm}R_{1c\pm}}\\
&+\frac{L_cM'^2(R^2_{1b\pm}+R^2_{1c\pm})\cos(L_bR_{1b\pm})\cos(L_cR_{1c\pm})\sin(L_aR_{1a\pm})}{R^2_{1c\pm}R_{1a\pm}}\\
&+\frac{L_cM'^2(R^2_{1b\pm}+R^2_{1c\pm})\cos(L_aR_{1a\pm})\cos(L_cR_{1c\pm})\sin(L_bR_{1b\pm})}{R^2_{1c\pm}R_{1b\pm}}\\
&-\frac{M'^2M''^2(R^2_{1a\pm}+R^2_{1b\pm})\cos(L_cR_{1c\pm})\sin(L_aR_{1a\pm})\sin(L_bR_{1b\pm})}{R^3_{1a\pm}R_{1b\pm}}\\
&-\frac{M'^2M''^2(R^2_{1a\pm}+R^2_{1c\pm})\cos(L_bR_{1b\pm})\sin(L_aR_{1a\pm})\sin(L_cR_{1c\pm})}{R^3_{1a\pm}R_{1c\pm}}\\
&-\frac{M'^2M''^2(R^2_{1a\pm}+R^2_{1b\pm})\cos(L_cR_{1c\pm})\sin(L_aR_{1a\pm})\sin(L_bR_{1b\pm})}{R^3_{1b\pm}R_{1a\pm}}\\
&-\frac{M'^2M''^2(R^2_{1b\pm}+R^2_{1c\pm})\cos(L_aR_{1a\pm})\sin(L_bR_{1b\pm})\sin(L_cR_{1c\pm})}{R^3_{1b\pm}R_{1c\pm}}\\
&-\frac{M'^2M''^2(R^2_{1a\pm}+R^2_{1c\pm})\cos(L_bR_{1b\pm})\sin(L_aR_{1a\pm})\sin(L_cR_{1c\pm})}{R^3_{1c\pm}R_{1a\pm}}\\
&-\frac{M'^2M''^2(R^2_{1a\pm}+R^2_{1b\pm})\cos(L_aR_{1a\pm})\sin(L_bR_{1b\pm})\sin(L_cR_{1c\pm})}{R^3_{1c\pm}R_{1b\pm}}\\
&-\frac{L_aM'^2(R^2_{1b\pm}+R^2_{1c\pm})\sin(L_aR_{1a\pm})\sin(L_b1b\pm)\sin(L_cR_{1c\pm})}{R_{1a\pm}R_{1b\pm}R_{1c\pm}}\\
&-\frac{L_bM'^2(R^2_{1a\pm}+R^2_{1c\pm})\sin(L_aR_{1a\pm})\sin(L_b1b\pm)\sin(L_cR_{1c\pm})}{R_{1a\pm}R_{1b\pm}R_{1c\pm}}\\
&-\frac{L_cM'^2(R^2_{1a\pm}+R^2_{1b\pm})\sin(L_aR_{1a\pm})\sin(L_b1b\pm)\sin(L_cR_{1c\pm})}{R_{1a\pm}R_{1b\pm}R_{1c\pm}}.
\end{aligned}
\tag{D.3}
$$

Appendix E

Principal Axis Transformation

Here we show a principle axis transformation of a second order curve with the general form

$$ax^2 + 2bxy + cy^2 + 2dx + 2ey + f = 0. \tag{E.1}$$

Since in our theory we have elliptically shaped hole pockets, we can restrict ourselves to the case of an ellipsis. Defining

$$A = \det \begin{pmatrix} a & b & d \\ b & c & e \\ d & e & f \end{pmatrix}, \quad B = \det \begin{pmatrix} a & b \\ b & c \end{pmatrix}, \tag{E.2}$$

we then obtain the normal form of an ellipse

$$a'x'^2 + c'y'^2 + \frac{A}{B} = 0, \tag{E.3}$$

with

$$a' = \frac{a + c + \sqrt{(a-c)^2 + 4b^2}}{2}, \quad c' = \frac{a + c - \sqrt{(a-c)^2 + 4b^2}}{2}. \tag{E.4}$$

In order to calculate the fermion density $n^f_\pm$ and the kinetic energy density $t^f_\pm$ of one specific hole pocket $P^f_\pm$, it is necessary to rotate the ellipse of the pocket according to the directions above. In the expansion according to eq.(4.30), the ellipse is described by

$$-\left(\frac{\partial f^f_\pm}{\partial E^f_\pm}\right)^{-1}\left(\frac{1}{2}\frac{\partial^2 f^f_\pm}{\partial q^2}q^2 + \frac{1}{2}\frac{\partial^2 f^f_\pm}{\partial q_2^2}p_2^2 + \frac{\partial^2 f^f_\pm}{\partial q \partial p_2}qp_2\right) - T^f_\pm = 0 \tag{E.5}$$

Thus, we have

$$A^f_\pm = \det \begin{pmatrix} a^f_\pm & b^f_\pm & 0 \\ b^f_\pm & c^f_\pm & 0 \\ 0 & 0 & f^f_\pm \end{pmatrix}, \quad B^f_\pm = \det \begin{pmatrix} a^f_\pm & b^f_\pm \\ b^f_\pm & c^f_\pm \end{pmatrix}. \tag{E.6}$$

With

$$a^f_\pm = -\frac{1}{2}\frac{\partial^2 f^f_\pm}{\partial q^2}\left(\frac{\partial f^f_\pm}{\partial E^f_\pm}\right)^{-1},$$

$$
\begin{aligned}
b^f_\pm &= -\frac{1}{2}\frac{\partial^2 f^f_\pm}{\partial q\ \partial p_2}\left(\frac{\partial f^f_\pm}{\partial E^f_\pm}\right)^{-1}, \\
c^f_\pm &= -\frac{1}{2}\frac{\partial^2 f^f_\pm}{\partial q^2}\left(\frac{\partial f^f_\pm}{\partial E^f_\pm}\right)^{-1}, \\
f^f_\pm &= -T^f_\pm. \qquad \text{(E.7)}
\end{aligned}
$$

This gives us the coefficients of the ellipse after the principal axis transformation

$$
\begin{aligned}
\frac{A^f_\pm}{B^f_\pm} &= -T^f_\pm \\
a'^f_\pm &= -\frac{1}{4}\left(\frac{\partial f^f_\pm}{\partial E^f_\pm}\right)^{-1}\left(\frac{\partial^2 f^f_\pm}{\partial q^2}+\frac{\partial^2 f^f_\pm}{\partial p_2^2}-\sqrt{\left(\frac{\partial^2 f^f_\pm}{\partial p_2^2}-\frac{\partial^2 f^f_\pm}{\partial q^2}\right)^2+4\frac{\partial^2 f^f_\pm}{\partial q\ \partial p_2}}\right) \\
c'^f_\pm &= -\frac{1}{4}\left(\frac{\partial f^f_\pm}{\partial E^f_\pm}\right)^{-1}\left(\frac{\partial^2 f^f_\pm}{\partial q^2}+\frac{\partial^2 f^f_\pm}{\partial p_2^2}+\sqrt{\left(\frac{\partial^2 f^f_\pm}{\partial p_2^2}-\frac{\partial^2 f^f_\pm}{\partial q^2}\right)^2+4\frac{\partial^2 f^f_\pm}{\partial q\ \partial p_2}}\right). \qquad \text{(E.8)}
\end{aligned}
$$

Hence, the normalized transformed ellipse of a hole pocket $P^f_\pm$ reads

$$
\frac{a'^f_\pm}{T^f_\pm}q'^2+\frac{c'^f_\pm}{T^f_\pm}p'^2_2=1. \qquad \text{(E.9)}
$$

This is the form we used to calculate the fermion density $n^f_\pm$ and the kinetic energy density $t^f_\pm$ of a hole pocket $P^f_\pm$.

Bibliography

[1] J. Gasser and H. Leutwyler, *Chiral Perturbation Theory: Expansions in the Mass of the Strange Quark*, Nucl. Phys. **B250**, 465 (1985).

[2] S. Chakravarty, D. R. Nelson and B. I. Halperin, *Low temperature behavior of two-dimensional quantum antiferromagnets*, Phys. Rev. Lett. **60**, 1057–1060 (1988).

[3] A. Damascelli, Z. Hussain and Z. X. Shen, *Angle-resolved photoemission studies of the cuprate superconductors*, Rev. Mod. Phys. **75**, 473 (2003).

[4] F. Kämpfer, M. Moser and U.-J. Wiese, *Systematic Low-Energy Effective Theory for Magnons and Charge Carriers in an Antiferromagnet*, Nucl. Phys. **B729**, 317–360 (2005).

[5] C. Brügger, F. Kämpfer, M. Moser, M. Pepe and U.-J. Wiese, *Two-Hole Bound States from a Systematic Low-Energy Effective Field Theory for Magnons and Holes in an Antiferromagnet*, Phys. Rev. **B74**, 224432 (2006).

[6] P. Hasenfratz and H. Leutwyler, *Goldstone Boson Related Finite Size Effects in Field Theory and Critical Phenomena with O(n) Symmetry*, Nucl. Phys. **B343**, 241–284 (1990).

[7] P. Hasenfratz and F. Niedermayer, *Finite size and temperature effects in the AF Heisenberg model*, Z. Phys. **B92**, 91 (1993).

[8] D. S. Fisher, *Universality, low-temperature properties, and finite-size scaling in quantum antiferromagnets*, Phys. Rev. B **39**, 11783 (1989).

[9] H. Neuberger and T. Ziman, *Finite-size effects in Heisenberg antiferromagnets*, Phys. Rev. B **39**, 2608–2618 (1989).

[10] V. Kotov and O. Sushkov, *Stability of the spiral phase in the 2D extended t-J model*, Phys. Rev. **B 70**, 195105 (2004).

[11] O. Sushkov and V. Kotov, *Superconducting Spiral Phase in the Two-Dimensional t-J Model*, Phys. Rev. **B 70**, 024503 (2004).

[12] B. Shraiman and E. Siggia, *Spiral Phase of a Doped Quantum Antiferromagnet*, Phys. Rev. Lett. **62**, 1564 (1989).

[13] C. Brügger, C. P. Hofmann, F. Kämpfer, M. Pepe and U.-J. Wiese, *Homogeneous versus Spiral Phases of Hole-doped Antiferromagnets: A Systematic Effective Field Theory Investigation*, Phys. Rev. **B75**, 014421 (2007).

[14] F. Kämpfer, *Effective Field Theory for Charge Carriers in an Antiferromagnet*, Masters Thesis, Universität Bern (2005).

[15] M. Moser, *Effective Field Theory for Charge Carriers in an Antiferromagnet*, Dissertation, Universität Bern (2006).

[16] C. Bolliger, *Fermion Simulation in the t-J Model*, Masters Thesis, Universität Bern (2006).